Sea Ice Climate Change Initiative: Phase 1

ANT D1.8 Antarctic Sea Ice Thickness Retrieval & Assessment

Doc Ref: SICCI-ANT-SITRA-06-15

Version: 1 Pr1

Date: 19th June 2015

Change Record

Issue	Date	Reason for Change	Author
1.0	June 22 2015	First draft	Stefan Kern
1.0	June 25 2015	Second draft, only discussion and conclusion missing	Stefan Kern
1.0	June 30 2015	Final version	Stefan Kern

Authorship

Role	Name	Signature
Written by:	S. Kern (UH)	
Checked by:	G. Timms (CGI)	
Approved by:	S. Sandven (NERSC)	
Authorised by:	P. Lecomte (ESA)	

Distribution

Organisation	Names	Contact Details
ESA	Pascal Lecomte	Pascal.Lecomte@esa.int
NERSC	Stein Sandven, Natalia Ivanova, Kirill Khvorostovsky	Stein.Sandven@nersc.no; natalia.ivanova@nersc.no; kirill.khvorostovsky@nersc.no
CGI	Gary Timms, Sabrina Mbajon, Clive Farquhar	gary.timms@cgi.com; sabrina.mbajon.njiche@cgi.com; clive.farquhar@cgi.com
MET Norway	Thomas Lavergne, Atle Sørensen	t.lavergne@met.no; atlems@met.no
DMI	Leif Toudal Pedersen, Rasmus Tonboe	ltp@dmi.dk; rtt@dmi.dk
DTU	Roberto Saldo, Henriette Skourup	rs@space.dtu.dk; mailto:hsk@space.dtu.dk
FMI	Marko Mäkynen, Eero Rinne	marko.makynen@fmi.fi; eero.rinne@fmi.fi;
University of Hamburg	Stefan Kern	stefan.kern@zmaw.de;
University of Bremen	Georg Heygster	heygster@uni-bremen.de
MPI-M	Dirk Notz, Felix Bunzel	dirk.notz@zmaw.de; felix.bunzel@mpimet.mpg.de

Organisation	Names	Contact Details
Ifremer	Fanny Ardhuin	Fanny.Ardhuin@ifremer.fr
AWI	Marcel Nicolaus, Stefan Hendricks, Sandra Schwegmann, Thomas Hollands	marcel.nicolaus@awi.de; stefan.hendricks@awi.de; sandra.schwegmann@awi.de; thomas.hollands@awi.de

Table of Contents

1 Introduction ... 7
- 1.1 Purpose ... 7
- 1.2 Scope ... 7
- 1.3 Document Structure ... 7
- 1.4 Document Status ... 7
- 1.5 Document Introduction ... 7
- 1.6 Applicable Documents ... 8
- 1.7 Applicable Standards ... 8
- 1.8 Reference Documents ... 8
- 1.9 Acronyms and Abbreviations ... 9

2 Data Sources ... 10
- 2.1 Laser Altimeter data ... 10
- 2.2 Radar Altimeter data ... 11
- 2.3 Snow Depth data ... 11
- 2.4 Sea ice concentration data ... 12

3 Methods ... 13
- 3.1 ICESat ... 13
- 3.2 Envisat RA2 and CryoSat-2 ... 16

4 Results ... 18
- 4.1 ICESat-1 only ... 18
- 4.2 Comparison ICESat-1 to Envisat RA2 ... 33
- 4.3 Comparison Envisat RA2 to CryoSat-2 ... 41
- 4.4 Discussion of the results ... 48

5 Summary ... 59

6 Literature ... 61

List of Figures

Es konnten keine Einträge für ein Abbildungsverzeichnis gefunden werden.

List of Tables

Table 1-1: Applicable Documents 8

Table 1-2: Applicable Standards 8

Table 1-3: Reference Documents 8

Table 1-4: Acronyms 9

1 Introduction

1.1 Purpose

This document reports on the work done for Work Package WP 1300 of the ESA CCI Sea ice ECV Project Option: Antarctic sea ice thickness distribution. The main goal of this WP is to assess and eventually combine the freeboard data provided by the other partners from other sensors within WP 1200.

1.2 Scope

This document gives an assessment about some different retrieval possibilities for sea ice thickness using satellite altimeter freeboard measurements.

1.3 Document Structure

After this introduction the data used will be described in Section 2. Section 3 gives a description of the methods used. Section 4 shows the results and section 5 summarizes the results.

1.4 Document Status

This is the final issue 1 version of this report.

1.5 Document Introduction

This report aims to briefly describe the different approaches used to derive sea ice thickness information from freeboard information obtained from satellite altimetry. The methodology and limitations of the derivation of freeboard data used for this report is described in RD-3, RD-4 and RD-5.

We not that we distinguish between two forms of freeboard. One it the sea ice freeboard. This is the elevation of the sea ice surface relative to the sea surface. A sea ice freeboard can be negative – in those cases when the ice surface is suppressed below the water line because of a heavy snow load, for example. The other is the so-called sea ice+snow or: total freeboard. This is the elevation of the snow surface relative to the sea surface. In contrast to the sea ice freeboard the total freeboard is always positive.

The total freeboard is typically the quantity which can be measured by a (satellite) laser altimeter such as the one on ICESat-1 (RD-3). The sea ice freeboard is the quantity which is supposed to be measured by a (satellite) radar altimeter. In theory, at the frequencies used by a radar altimeter, which lie usually in the Ku-Band (12-18 GHz), radar waves penetrate the dry snow on top of the sea ice and see the ice snow interface of sea ice surface as the main reflecting horizon and hence are supposed to obtain information about the sea ice freeboard. Whether and how well this assumption is met in the data set used here is given in RD-4 and RD-5.

1.6 Applicable Documents

The following table lists the Applicable Documents that have a direct impact on the contents of this document.

Acronym	Title	Reference	Issue
AD-01	Sea Ice ECV Project Management Plan	ESA-CCI_SICCI_PMP_D6.1_v1.1	1.1
AD-02	ESA-SICCI Scientific user consultation and detailed specification: Statement of Work (SoW)	EOP-SEP/SOW/0031-09/SP	1.4.2
AD-03	Annex top the SoW	EOP-SEP/SOW/0031-09/SP	1.4.2

Table 1-1: Applicable Documents

1.7 Applicable Standards

Acronym	Title	Reference	Issue

Table 1-2: Applicable Standards

1.8 Reference Documents

Acronym	Title	Reference	Issue
RD-01	SICCI_URD	SICCI-URD-03-12	1.3
RD-02	SICCI_ATB D	SICCI-Ant-SD-AS-14-04	1.0
RD-03	D1.6 ICESat ANT Freeboard	SICCI-ICESatANT-14-03	1.0
RD-04	D1.4 Report on Envisat RA2 Antarctic freeboard retrieval and assessment	SICCI-RERA2AFRA-12-14	1.1
RD-05	D1.5 Report on Cryosat-2 Antarctic freeboard retrieval and assessment	SICCI-RCS2AFRA-10-14	1.1
RD-06	D1.1 Passive microwave snow depth on Antarctic sea ice assessment	SICCI-Ant-PMW-SDASS-11-14	1.1
RD-07	ANT D1.3 Snow depth data set v1.1 product user guide	SICCI-ANT-SD-PUG-14-08	2.0
RD-08	D1.2 ANT snow depth from alternative sources	SICCI-ANT-SD-AS-14-04	1.0
RD-09	D4.1 Product validation and intercomparison report (PVIR)	SICCI-PVIR	1.1

Table 1-3: Reference Documents

1.9 Acronyms and Abbreviations

Acronym	Meaning
EO	Earth Observation
PDGS	Payload Data Ground System

Table 1-4: Acronyms

2 Data Sources

This section provides the overview about the data sources used for the results presented in this report.

These are without exclusion based on satellite data: laser altimeter data from the Geoscience Laser Altimeter System (GLAS) aboard the Ice, Cloud and Elevation Satellite ICESat-1; radar altimeter data from the RA-2 Environmental Satellite Envisat and from the SIRAL instrument aboard the CryoSat-2 satellite [RD-03; RD-04; RD-05].

In addition sea ice concentration data computed from satellite microwave radiometry: SSM/I, SSM/IS and AMSR-E are used [Kaleschke et al., 2001; Spreen et al., 2008; Kern et al., 2010].

Satellite microwave radiometry of the AMSR-E is also the data source for the snow depth data used [RD-06; RD-07; Markus and Cavalieri, 1998; Comiso et al., 2003; Cavalieri et al., 2004].

Generally the sea ice thickness is computed from the freeboard here following Archimedes Principle assuming the sea ice is freely floating at the sea surface. In this case the freeboard can be combined with information about sea ice, snow, and water density, and snow depth to compute the sea ice thickness as will be detailed in Section 3.

2.1 Laser Altimeter data

We use GLAS/ICESat L2 sea-ice altimetry data (GLA13) of release 33 [Zwally et al., 2011]. The data are downloaded for ICESat measurement periods 2B to 2J from the U.S. National Snow and Ice Data Center (NSIDC): http:nsidc.org/data/gla13.html). This data is used to compute Antarctic wide distribution of the total freeboard as described in RD-03; see also Kern and Spreen [2015]. Maps of the total freeboard at 25 km grid resolution and at 100 km grid resolution are computed separately and are available as an average for each ICESat period from 2B (February/March 2004 or FM04) to 3J (February/March or FM08) for the freeboard-to-thickness conversion (see Table 2.1). Note that data need to be averaged over such long periods – about 33-35 days long – to obtain a sufficiently dense coverage with valid data. In addition maps of the freeboard retrieval uncertainty are computed and are used in this report to compute sea ice thickness retrieval uncertainty. Sample maps of the total freeboard and the total freeboard uncertainty are given in RD-03.

Table 2.1: ICESat measurement periods used. The naming convention in the text is given by the season abbreviation, e.g. “ON” followed by the two last digits of the year, e.g. “04”, so that “spring 2004” reads “ON04” and “winter 2006” reads “MJ06”.

Year	Spring (ON)	Fall (FM)	Winter (MJ)
2004	Oct. 3 – Nov. 8	Feb. 17 – Mar. 21	May 18 – June 21
2005	Oct. 21 – Nov. 24	Feb. 17 – Mar. 24	May 20 – June 23
2006	Oct. 25 – Nov. 27.	Feb. 22 – Mar. 27	May 24 – June 26
2007	Oct. 2 – Nov. 5	Mar. 12 – Apr. 14	--
2008	--	Feb. 17 - Mar.	--

For inter-comparison purposes we downloaded the gridded total freeboard and sea ice thickness estimates published by Kurtz and Markus [2012] (see also [Markus et al., 2011]) from the Cryosphere Science Research Portal at NASA: http://seaice.gsfc.nasa.gov/csb/index.php?section=272). This data set contains total freeboard estimates based on the approach described in Markus et al. [2011] as well as sea ice thickness estimates (see Section 3 for details)

2.2 Radar Altimeter data

We used radar freeboard data obtained from Envisat RA-2 [RD-04] and from CryoSat-2 [RD-05].

The Envisat RA2 data are provided on an EASE2-grid with 100 km grid resolution. For our investigation we re-project all RA2 freeboard data used to the NSIDC polar-stereographic grid of the southern hemisphere with 100 km grid resolution and minimum distortion at 70°S.

Envisat RA2 freeboard data are used as ICESat-period mean values (see Section 2.1) for periods 2B to 3J [RD-04]. Only the freeboard data given in this ESA SICCI data product of WP 1200 are used. Uncertainty information is not provided. The number of valid data which is provided along with the data could be used as a quality criterion but has not been included to maximize the number of the data to compute SIT from. In addition to these ICESat-period mean freeboard data also monthly average freeboard is used for 2011 for months January to September because this is the overlap period between Envisat RA2 and CryoSat-2 when also snow depth data for SIT retrieval are available (see Section 2.3).

CryoSat-2 (CS-2) data are provided as monthly average freeboard on an EASE2-grid with 25 km grid resolution [RD-05]. For our investigation we re-project all CS-2 freeboard data used to the NSIDC polar-stereographic grid of the southern hemisphere with 100 km grid resolution and minimum distortion at 70°S.

In contrast to Envisat RA2 freeboard data CS-2 freeboard data come together with uncertainty information. However, in order to be compatible to the Envisat RA-2 data we did not take this parameter into account when computing the SIT uncertainty based on CS-2 and RA2 data.

2.3 Snow Depth data

The snow depth distribution required to convert freeboard into SIT is taken from the AMSR-E snow depth data set [Cavalieri et al., 2004]. This data comes daily as 5-day mean values for 2002 to September 2011. This data does not include any uncertainty information. For the SIT retrieval based on ICESat and the contemporary Envisat RA2 data the snow depth data were re-projected from 12.5 km NSIDC polar-stereographic grid true at 70°S to the corresponding grid with 25 km and 100 km grid resolution for ICESat measurement periods 2B to 3J.

For the SIT computation of the period with contemporary RA2 and CS-2 data we used the re-processed AMSR-E snow depth data set [RD-06; RD-07]. These snow depth data are provided as a monthly climatology with uncertainty estimates at 25 km grid resolution. For our analysis this data is also re-projected to the corresponding 100 km grid. The snow depth uncertainty provided together with the product is quite small and does not reflect the potential biases and variations in snow depth due to weather effects [see RD-08]. Hence instead of the retrieval uncertainty we used the temporal snow depth standard deviation per 25 km grid cell as a measure of the uncertainty.

As the evaluation of the re-processed AMSR-E snow depth product is still ongoing we decided that it would be justified more to use the well-known NSIDC snow depth product for the computation of SIT for the ICESat-period – as we also intended to release this as an Antarctic sea ice thickness prototype product – while we keep usage of the new AMSR-E snow depth product for the more experimental freeboard-to-thickness conversion of the RA2 to CS-2 overlap period with AMSR-E data.

2.4 Sea ice concentration data

Basically all products used in this report include a different sea ice concentration (SIC) data set.

The ICESat freeboard product used includes the daily 5-day median-filtered ARTIST Sea Ice (ASI) algorithm sea ice concentration data set provided as a co-production from IFREMER and UHAM: http://icdc.zmaw.de/1/daten/cryosphere/seaiceconcentration-asi-ssmi.html [Kaleschke et al., 2001; Kern et al., 2010]. In the freeboard retrieval and also later in the freeboard-to-thickness conversion only SIC > 60% is used.

The Envisat RA2 freeboard product utilizes the NSIDC SIC CDR [Meier et al., 2006] provided on NSIDC 25 km grid resolution polar-stereographic grid.

The CS-2 freeboard product utilizes the Eumetsat OSI-SAF SIC product OSI-403 sea ice concentration on 10 km grid resolution NSIDC polar-stereographic grid.

Finally, the snow depth data sets utilize different snow depth data sets. While AMSR-E snow depth data provided by NSIDC [Cavalieri et al., 2004] is based on AMSR-E NASA-Team 2 algorithm SIC data at 12.5 km ggrid resolution, the SICCI AMSR-E snow depth data provided by UB [RD-06; RD-07] utilize ASI-algorithm SIC data computed from AMSR-E data at 6.25 km grid resolution [Spreen et al., 2008].

3 Methods

This section gives an overview about the methods used to convert freeboard – either total freeboard or sea ice freeboard – to sea ice thickness.

Freeboard, sea ice concentration and snow depth are considered here as given data and the methodologies to derive these parameters is not given. We refer to section 2 for the relevant references.

The approaches listed in sub-section 3.1 and 3.2 require densities of water, sea ice and snow. Unless stated otherwise the following densities are used [Yi et al., 2011]:

Open water: ρ_{water} = 1023.9 kg/m³, snow: ρ_{snow} = 300.0 kg/m³, sea ice: ρ_{ice} = 915.1 kg/m³.

Also, unless stated otherwise, the AMSR-E snow depth product of the NSIDC (see Section 2) is used.

3.1 ICESat

ICESat provides the total freeboard. Freeboard-to-thickness conversion approaches for ICESat have been developed for the Arctic [Kwok and Cunningham, 2008] and for the Antarctic [Zwally et al., 2008]. In the Antarctic, in contrast to the Arctic, sea ice can be flooded with sea water. This has implications for the sea ice thickness retrieval using laser altimetry.

3.1.1 SICCI approach

As suggested by Zwally et al. [2008] and confirmed by Yi et al. [2011] it seems to be practical to discriminate between cases with positive sea ice freeboard and cases with negative sea ice freeboard and hence flooded sea ice. As a criterion to decide whether sea ice freeboard is positive or negative the difference total freeboard F minus snow depth S is taken; if this difference is negative sea ice freeboard is assumed to be negative, if this difference is positive sea ice freeboard is assumed to be positive.

The SICCI approach follows the methods proposed by Zwally et al. [2008] and Yi et al. [2011] and computes the sea ice thickness I from F and S via the equations (1) and (2) depending on whether S is smaller than F (1) or S is larger than or equal to F (2). Note that Eq. 2 is independent of S.

$$F > S: I = F\frac{\rho_{water}}{\rho_{water}-\rho_{ice}} - S\frac{\rho_{water}-\rho_{snow}}{\rho_{water}-\rho_{ice}} \quad (1)$$

$$F \leq S: I = F\frac{\rho_{snow}}{\rho_{water}-\rho_{ice}} \quad (2)$$

Densities are taken as listed before subsection 3.1. As snow depth S the AMSR-E snow depth is used. Freeboard values above 1 m are discarded following Yi et al. [2011]. Equations (1) and (2) are applied to gridded freeboard data at 25 km and 100 km grid resolution.

Sea ice thickness retrieval uncertainties are computed using Gaussian Error propagation [Kern and Spreen, 2015; Spreen et al., 2006] applied to equations (1) and (2) resulting in Equations (3) and (4):

$$F > S: \sigma_I^2 = \left(dF\frac{\rho_{water}}{\rho_{water}-\rho_{ice}}\right)^2 + \left(dS\frac{\rho_{snow}-\rho_{water}}{\rho_{water}-\rho_{ice}}\right)^2 + \left(d\rho_{snow}\frac{S}{\rho_{water}-\rho_{ice}}\right)^2 + \left(d\rho_{ice}\frac{\rho_{water}F+\rho_{snow}S-\rho_{water}S}{(\rho_{water}-\rho_{ice})^2}\right)^2 \quad (3)$$

$$F \leq S: \sigma_I^2 = \left(dF\frac{\rho_{water}}{\rho_{water}-\rho_{ice}}\right)^2 + \left(d\rho_{snow}\frac{F}{\rho_{water}-\rho_{ice}}\right)^2 + \left(d\rho_{ice}\frac{\rho_{water}F}{(\rho_{water}-\rho_{ice})^2}\right)^2 \quad (4)$$

The contribution of the uncertainty in water density is considered small compared to the contributions of the other parameters and is therefore neglected. As uncertainties for snow and sea ice density we use $d\rho_{snow}$ = 50 kg/m³ and $d\rho_{ice}$ = 20 kg/m³ (see [Maksym and Markus, 2008])

As uncertainty of the snow depth we use dS = 0.3 x S. This is a rather conservative estimate – particularly when considering 100 km grid resolution data. However, the fact that snow depth products from satellite microwave radiometry are potentially biased low over deformed sea ice, that these products do not come with an uncertainty information, and that the new snow depth product from SICCI [RD-06, RD-07] is not yet validated enough motivated us to choose such a conservative snow depth uncertainty (see also [Kern and Spreen, 2015]).

As uncertainty for freeboard we use dF = 3 x dF', dF' = freeboard retrieval uncertainty. The motivation for multiplying the freeboard retrieval uncertainty with a factor of 3 is given and discussed in Kern and Spreen [2015].

3.1.2 *Kurtz and Markus (KandM) approach*

In RD-03 as well as in Kern and Spreen [2015] the approach of Kurtz and Markus [2012] (abbreviated KandM) is introduced and discussed. This approach differs in several ways from the SICCI approach.

First the freeboard retrieval is slightly different and results in slightly smaller overall mean total freeboard for the Weddell Sea: 0.06 m when averaged over all 3 ICESat periods per year for 2004 to 2006 [Kern and Spreen, 2015]; also for the entire Antarctic SICCI freeboard tends to be higher than KandM freeboard with modal values being 0.05 to 0.1 m higher for basically all periods investigated [RD-03].

Secondly, the freeboard-to-thickness conversion assumes zero sea ice freeboard everywhere [Kurtz and Markus, 2012]. This way the discrimination between positive and negative sea ice freeboard cases based on satellite-based snow depth measurements is avoided; this could be an advantage (see Section 4.4). As another advantage, setting the sea ice freeboard to zero implies that the measured total freeboard equals the snow depth. Hence a separate snow depth data set is not required to convert freeboard to thickness using the KandM approach.

Third, values of sea ice density and snow density are chosen to vary seasonally. For MJ and ON periods sea ice density is 900 kg/m³ and for FM period the value chosen is 875 kg/m³. Snow densities are 320 kg/m³, 350 kg/m³, and 340 kg/m³ for ON, FM, and MJ periods.

3.1.3 Empirical approaches from in-situ measurements (OC2013)

By using in-situ observations of sea ice thickness, snow depth and freeboard from 15 research cruises into the Southern Ocean Ozsoy-Cicek et al. [2013] (abbreviated OC2013) proposed empirical relationships which allow direct conversion of the total freeboard into sea ice thickness without the need for additional snow depth and density information. This could be a great advantage compared to the previous two approaches.

We test this approach as follows: OC2013 derived empirical relationships, i.e. a set of linear regression coefficients, for five different regions in the Southern Ocean: Western Weddell Sea (WWS), Eastern Weddell Sea, Eastern Antarctic (EA), Ross Sea, and Bellingshausen-Amundsen Sea. From these relationships we pick two: WSW and EA because for WSW the relationship can be expected to be dominated by perennial sea ice and because both regions, WSW and EA, showed the most extreme values of the five regions investigated. In addition to these two sets of regression coefficients we computed an overall Antarctic (AAall) set of regression coefficients. These three sets are given together with the uncertainty estimates of the coefficients (see [Ozsoy-Cicek et al., 2013]) in Table 3.1.

Table 3.1: Slope and intercept values of the three selected linear regressions for Western Weddell Sea (WWS), Eastern Antarctic (EA) and the entire Antarctic (AAall) together with rather conservative uncertainty estimates for slope and intercept of the two single regions. For region AAall the uncertainty estimate is based on the average slope and intercept uncertainties of all five regions. Intercept and intercept error are given in centimeters.

Region	Slope: a	Slope error: da	Intercept: b	Intercept error: db
WWS	2.34	0.3 x a	22.0	10.0
EA	3.50	0.3 x a	26.0	10.0
AAall	2.77	3 x 0.45	20.7	3 x 3.6

Based on these regressions sea ice thickness I and its uncertainty σ_I are computed (in meters) as follows:

$$I = 0.01\,(b + a\,F) \tag{5}$$

$$\sigma_I = 0.01\,\sqrt[2]{(a\,dF)^2 + (F\,da)^2 + (db)^2} \tag{6}$$

3.1.4 SICCI approach with SSM/I snow depth climatology (MandC)

Instead of using daily – or in our case – monthly varying snow depth data of perhaps inferior quality one could use snow depth climatology. This is tested in this part. The SICCI freeboard and freeboard-to-thickness conversion is applied (Equations 1 and 2) but instead of using AMSR-E snow depth we use the mean all-Antarctic snow depth climatology given in Markus and Cavalieri [1998]. So all other parameters except the snow depth are the same as described in subsection 3.1.1 but the following snow depths are used and held fixed over space and time: 23 cm for FM periods and 13 cm for periods MJ and ON.

3.1.5 Replacing snow depth by varying sea ice density (Worby)

Another approach to get rid of the problem of a potentially biased snow depth from satellite microwave radiometry would be to completely omit usage of snow depth data and instead treat the sea ice – snow system as one layer with reduced density. Sea ice and snow densities from observations which are needed for this approach are taken from Worby et al. [2008]. The sea ice density is modified as follows:

$$\rho_{ice}^{*} = \frac{R\,\rho_{ice} + \rho_{snow}}{R+1} \tag{7}$$

with R being a seasonally dependent factor modifying the sea ice density. R is computed as the ratio between sea ice thickness and snow depth. The idea behind this is that the density of the one-layer system has to modify with the ratio between snow depth and ice thickness. Following Worby et al. [2008] the mean autumn (our FM periods), winter and spring average, i.e. including the contribution from ridged ice, sea ice thickness I is 0.68 m, 0.66 m and 0.81 m, respectively; the respective mean snow depth S is 0.10 m, 0.11 m, and 0.15 m, respectively. This results in R values of 6.8, 6.0, and 5.4 for fall, winter, and spring, respectively, which in turn translates into apparent ice densities $\rho_{ice}^{*}$of: 836 kg/m³, 827 kg/m³, and 819 kg/m³. Note that these are not the "real" sea ice density as are used by Kurtz and Markus [2012], see subsection 3.1.2, but density of a layer which incorporates the snow layer on top.

The sea ice thickness is then computed via:

$$I = F\,\frac{\rho_{water}}{\rho_{water} - \rho_{ice}^{*}} \tag{8}$$

3.2 Envisat RA2 and CryoSat-2

Sea ice thickness is computed from the radar freeboard provided by Envisat RA2 and CryoSat-2 in two ways. Theoretically these radar altimeters are supposed to sense the ice snow interface – hence the sea ice freeboard. However, there is evident in the literature as well as from the work reported in [RD-05] that this is not the case and that the radar altimeter return might actually come from the snow surface. Because of this potential ambiguity we decided to compute the sea ice thickness here int two different ways.

For one approach we assume that the radar freeboard is the sea ice freeboard. In this case the sea ice thickness is computed via:

$$I = \frac{(\rho_{snow}\,S + \rho_{ice}\,F)}{\rho_{water} - \rho_{ice}} \tag{9}$$

In Equation (9) all parameters except F are similar to those used in Equations (1) and (2) for the SICCI SIT retrieval using ICESat freeboard.

For the second approach we assume that the radar freeboard represents the total freeboard – as for ICESat. Here we simply apply Equations (1) and (2) for the sea ice thickness retrieval. Input parameters are similar to those described above.

Note that this applies to the computation of sea ice thickness from Envisat RA2 as far as it concerns the overlap periods with ICESat. For the months of overlapping CryoSat-2, Envisat RA2, and AMSR-E snow depth data we do not use the NSIDC snow depth product but the SICCI snow depth product generated at UB (see Section 2). This is the only difference though.

The sea ice uncertainty is computed via

$$\sigma_I^2 = \frac{1}{(\rho_{water} - \rho_{ice})^2}\left((dS\,\rho_{snow})^2 + (dF\,\rho_{water})^2 + (d\rho_{snow}\,S)^2 + \left(\frac{d\rho_{ice}\,(\rho_{snow}\,S + \rho_{water}\,F)}{\rho_{water} - \rho_{ice}}\right)^2\right) \tag{10}$$

for the case given by Equation (9), i.e. radar freeboard equals sea ice freeboard and using Equations (3) and (4) for the case that the radar freeboard represents the total freeboard.

In Equation (10) we have neglected the contribution by the open water density – similar to the sea ice thickness uncertainty computation for the SICCI approach (Equations 3 and 4). Uncertainties for snow and sea ice densities as well as for the snow depth are similar to those used in Equations (3) and (4). For the freeboard uncertainty dF we could choose none for Envisat RA2 and the one provided with the data set for CryoSat-2. But in order to have a similar uncertainty contribution for both types of sensor we set dF = 0.2*F.

The above-said is valid for the computation of the uncertainties for the ICESat – Envisat overlap period. For the overlap period with CryoSat-2 we used the temporal standard deviation of the SICCI snow depth instead of 3 * S as snow depth uncertainty.

4 Results

This section provides the results. We first start with looking at ICESat data only before we compare results from ICESat with those from Envisat RA2 (subsection 4.2) and results from Envisat RA2 with those from CryoSat-2 (subsection 4.3). Subsection 4.4 provides a further discussion of the results.

4.1 ICESat-1 only

4.1.1 SICCI versus KandM

The SICCI sea ice thickness and the sea ice thickness issued by Kurtz and Markus [2012] are the only available circum-Antarctic sea ice thickness products. Hence it makes sense to compare these two products first.

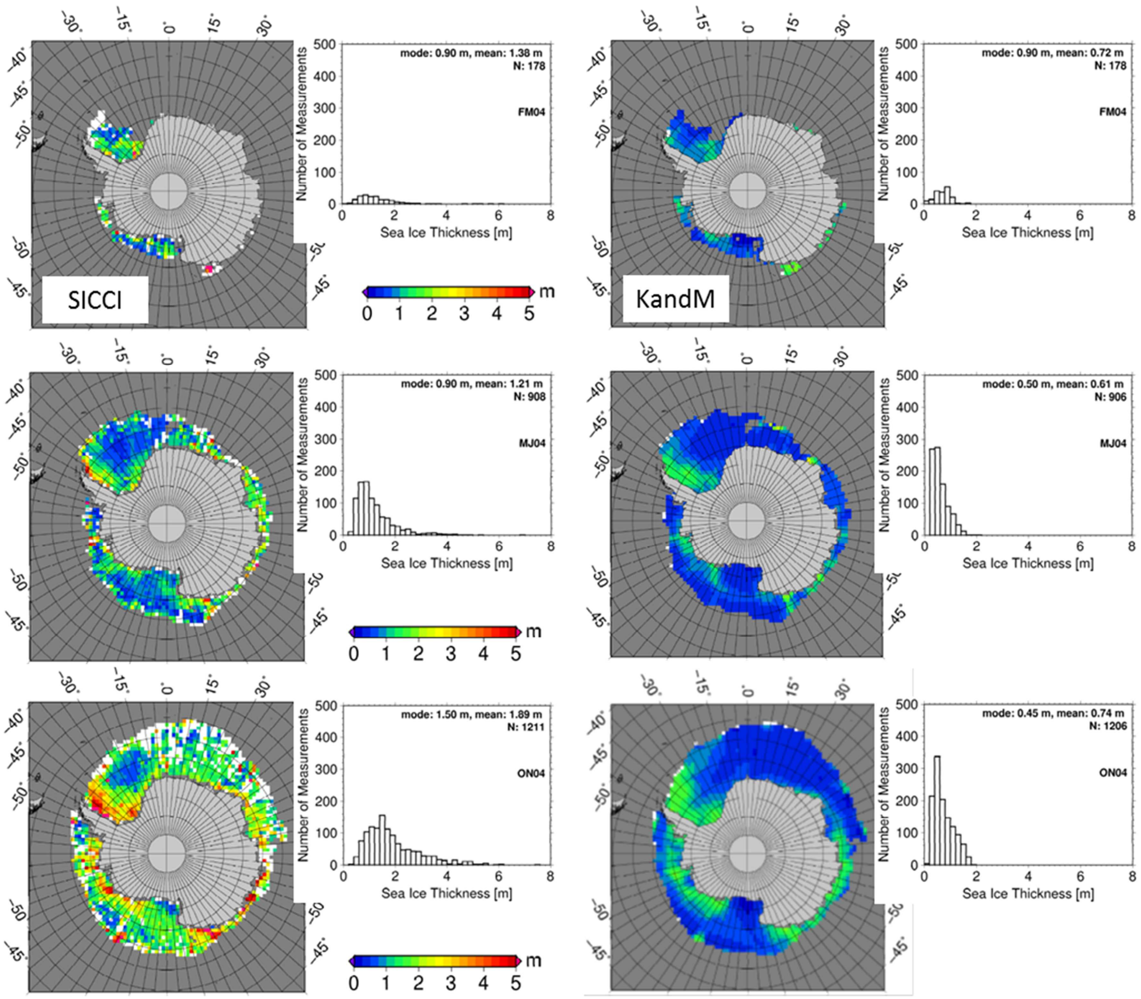

Figure 4.1: SICCI sea ice thickness distribution around the Antarctic from SICCI (left column) and from Kurtz and Markus [2012] (right column) for 2004. White areas in the maps show grid cells with sea ice but without enough valid sea ice thickness data. Grid cell size is 100 km. Only grid cells with a sea ice concentration above 60% are shown. Each map is accompanied by a histogram showing the sea ice thickness distribution using bins of 0.2 m width. ICESat periods FM04, MJ04 and ON04 are shown from top to bottom. In each histogram the modal and mean sea ice thickness is given together with the number of valid data points N.

Figure 4.1 illustrates the seasonal development in sea ice thickness as seen by ICESat. While in FM04 new ice barely started to form and hence most of the sea ice is relatively thick in MJ04 new ice formation has advanced around all of the Antarctic providing a wide belt of sea ice with thickness values between 0.5 m and 1.5 m. The most extensive zones of thinner sea ice are found in the central Weddell Sea and in most of the Ross and Amundsen Seas. Thicker sea ice is found along the East Antarctic coast, in some coastal areas in the Amundsen Sea and in the Weddell Sea. The latter is known for a substantial amount of perennial sea ice hugging the Antarctic Peninsula – as is demonstrated by the SICCI sea ice thickness map (see also [Yi et al., 2011]). From period MJ to period ON the amount of thicker sea ice increases while thin ice with values below 1 m stay mainly in the central Weddell Sea and in the southern Ross Sea where the area downstream of the Ross Ice Shelf polynya is known to be covered by thin sea ice. The sea ice distribution pattern in the Weddell Sea agrees well with the results of Yi et al. [2011].

The KandM sea ice thickness distribution tends to show similar features but differences between presumably perennial sea ice and seasonal sea ice are much smaller. In particular sea ice thickness values above 2 m are practically absent while the SICCI maps and histograms show a larger variability in sea ice thickness which seems to resemble what is known in terms of the Antarctic sea ice thickness distribution [Worby et al., 2008]. An encouraging result is the well-developed tail towards higher sea ice thickness values for period MJ and more so for period ON.

Note that Kurtz and Markus [2012] used kriging interpolation to fill gaps. SICCI sea ice thickness data are not interpolated.

Table 4.1: Modal sea ice thickness (SIT) from ICESat for all periods from FM 2004 to FM 2008 from the SICCI algorithm and the approach of Kurtz and Markus [2012], abbreviated KandM. The last two columns denote the average value of the 5, 3, and 4 periods for FM, MJ, and ON, respectively. The standard deviation given in the last two columns refers to the respective standard deviation. In these last two columns values in bold (italic) font are for 100 km (25 km) grid cell size.

Period	Year	2004	2005	2006	2007	2008	Mean ± Stdv	Mean ± Stdv
FM	SICCI	0.90	1.10	0.70	0.90	0.90	0.90 ± 0.14	*0.91 ± 0.19*
	KandM	0.90	1.10	0.70	0.75	0.75	0.85 ± 0.16	*0.76 ± 0.30*
MJ	SICCI	0.90	0.70	0.90	--	--	0.83 ± 0.12	*0.62 ± 0.14*
	KandM	0.50	0.50	0.30	--	--	0.43 ± 0.12	*0.43 ± 0.12*
ON	SICCI	1.50	1.30	1.50	1.30	--	1.40 ± 0.12	*1.38 ± 0.12*
	KandM	0.45	0.45	0.50	0.30	--	0.43 ± 0.09	*0.48 ± 0.03*

Table 4.2: As Table 4.1 but for the mean SIT.

Period	Year	2004	2005	2006	2007	2008	Mean ± Stdv	Mean ± Stdv
FM	SICCI	1.38	1.82	1.78	1.62	1.38	1.60 ± 0.21	*1.60 ± 0.29*
	KandM	0.72	1.01	0.94	0.71	0.70	0.82 ± 0.15	*0.83 ± 0.17*
MJ	SICCI	1.21	1.41	1.38	--	--	1.33 ± 0.11	*1.30 ± 0.09*
	KandM	0.61	0.69	0.60	--	--	0.63 ± 0.05	*0.65 ± 0.05*
ON	SICCI	1.89	1.84	1.94	1.78	--	1.86 ± 0.07	*1.90 ± 0.08*
	KandM	0.71	0.66	0.69	0.60	--	0.67 ± 0.05	*0.70 ± 0.06*

Tables 4.1 and 4.2 summarize the modal and the mean sea ice thickness obtained with the SICCI and the KandM approaches for all ICESat periods listed in Table 2.1. All columns but the last one are based on 100 km grid resolution.

Modal sea ice thickness from SICCI and KandM agree with each other within the temporal variability for FM periods. For the other periods an increasing difference can be observed with SICCI providing larger modal sea ice thickness than KandM, particularly for ON periods. Note that the modal sea ice thickness is more difficult to obtain and that especially for the FM period large differences from year to year can be caused by only a few more data in one bin compared to another bin.

Mean sea ice thickness from SICCI and KandM differ substantially all year round with SICCI always having larger mean sea ice thickness than KandM. On average one could say that the mean SICCI sea ice thickness is twice the mean KandM sea ice thickness.

We note that it does not make a difference for the mean sea ice thickness whether this comparison is carried out at 100 km grid resolution or at 25 km grid resolution: the last two columns in Table 4.2 reveal similar values and hence provide the same picture. This does not apply in the same extent to the modal sea ice thickness (Table 4.1) where the last two columns may differ. We address this, however, to the difficulty in deriving properly the modal sea ice thickness value from the histograms.

We note that even though FM period 2007 was later than all the other, actually covering March to April rather than February to March (Table 2.1), and even though ON-period 2007 was earlier than the other three ON periods (Table 2.1) these two periods do not show up with extreme values in the modal and mean sea ice thickness in Tables 4.1 and 4.2.

In order to figure out where the areas of greatest discrepancies are located in more detail we computed the difference SICCI minus KandM sea ice thickness. Figure 4.2 shows the differences in form of maps and corresponding histograms for ICESat periods in 2004. Maps and histograms illustrate that SICCI over-estimates sea ice thickness compared to KandM for basically most off the sea ice cover. There are some patches, however, where the difference SICCI minus KandM sea ice thickness is "around zero". Around zero means the difference is between -0.4 m and 0.4 m (pale blue and pale red in Figure 4.2). Note that 0.4 m is about the modal SICCI sea ice thickness uncertainty as will be shown later. These patches are located in the central to western Weddell Sea and in the outer Ross and Amundsen Seas in MY period and less extensive but still present in ON period in the same regions. Where these patterns of comparably small difference SICCI minus KandM sea ice thickness are located, changes from year to year (not shown).

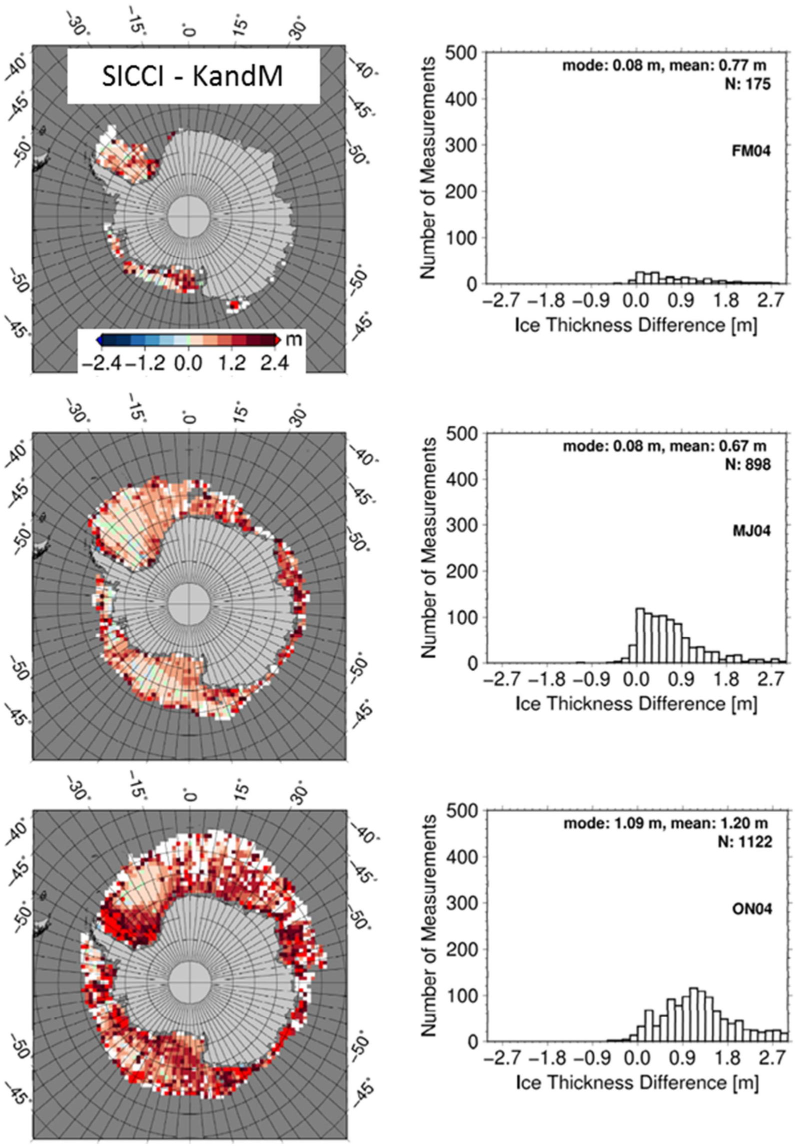

Figure 4.2: Difference SICCI minus KandM sea ice thickness for 2004. White areas in the maps show grid cells with sea ice but without enough valid sea ice thickness data. Grid cell size is 100 km. Only grid cells with a sea ice concentration above 60% are shown. Each map is accompanied by a histogram showing the sea ice thickness difference distribution using bins of 0.15 m width. ICESat periods FM04, MJ04 and ON04 are shown from top to bottom. In each histogram the modal and mean sea ice thickness difference is given together with the number of valid data points N.

Table 4.3 summarizes the SICCI minus KandM sea ice thickness differences for all ICESat periods listed in Table 2.1 together with the number of grid cells with valid data and with the mean of the differences for 100 km and 25 km grid resolution for all periods of one season, e.g. FM.

Table 4.3 reveals that for FM period modal sea ice thickness differences vary quite a lot between < 0.1 m and about 0.8 m while mean sea ice thickness differences stay quite close to 0.85 m for all years. This could again be explained with the difficulty to find an adequate modal value in the histograms for FM period due to the comparably low number of valid grid points – but also MJ periods show quite some variability in the modal sea ice thickness differences. MJ periods show similar mean sea ice thickness differences for 2004 to 2006. For ON periods the inter-annual variation in modal and mean sea ice thickness differences stays comparably small; also modal and mean sea ice thickness difference values differ less than for the other two periods. Overall one cans say that the modal and the mean difference SICCI minus KandM sea ice thickness stay similar for FM and MJ periods and increases for ON periods. Because the modal values is perhaps less representative we conclude here with the mean differences which are 0.84 m, 0.75 m, and 1.12 m for FM, MJ, and ON periods, respectively, which is close to the values one would read from Table 4.2: 0.78 m, 0.70 m, and 1.19 m.

Table 4.3: Modal and mean value of the difference SICCI minus KandM sea ice thickness (dSIT) for each period and, in last two columns, averaged over the 5, 3, and 4 ICESat periods in FM, MJ, and ON at 100 km grid resolution (normal font) and at 25 km grid resolution (italic font). The second value in the last two columns is the standard deviation of the respective values over the periods.

Period	Year	2004	2005	2006	2007	2008	Mean ± Stdv	Mean ± Stdv
FM	dSITmode	0.08	0.23	0.08	0.83	0.26	0.30 ± 0.31	*0.10 ± 0.01*
	dSITmean	0.77	0.87	0.87	0.87	0.85	0.84 ± 0.04	*0.59 ± 0.07*
	N	175	135	106	228	198	168 ± 49	*1422 ± 468*
MJ	dSITmode	0.08	0.08	0.53	--	--	0.23 ± 0.26	*0.13 ± 0.09*
	dSITmean	0.67	0.76	0.82	--	--	0.75 ± 0.08	*0.54 ± 0.05*
	N	898	905	936	--	--	913 ± 20	*8705 ± 613*
ON	dSITmode	1.09	0.98	1.24	1.16	--	1.12 ± 0.11	*0.81 ± 0.09*
	dSITmean	1.20	1.28	1.34	1.23	--	1.26 ± 0.06	*1.01 ± 0.03*
	N	1122	884	760	1145	--	978 ± 187	*6768 ± 1794*

Table 4.4 finally shows the all-period average of the modal and mean sea ice thickness difference SICCI minus KandM for 100 km and 25 km grid resolution. The difference is close to twice as large for the mean value when considering all ICESat periods listed in Table 2.1. In contrast to the mean sea ice thickness values shown in Table 4.2 it does make a difference whether 100 km or 25 km grid resolution is used because the average modal and mean sea ice thickness differences are smaller and also less variable for 25 km grid resolution. This is also evident in Table 4.3.

Table 4.4: All period mean of the modal and the mean value of the difference SICCI minus KandM sea ice thickness for 100 km (25 km) grid resolution in bold (italic) font.

	Mean ± Stdv	Mean ± Stdv
dSITmode	**0.55 ± 0.58**	*0.35 ± 0.40*
dSITmean	**0.96 ± 0.43**	*0.72 ± 0.35*

4.1.2 SICCI versus other alternative approaches

In this subsection we compare the SICCI sea ice thickness with the sea ice thickness obtained from ICESat data using different approaches. These are either new empirical ones, like the one from Ozsoy-Cicek et al. [2013] (OC2013), or a modification of the SICCI approach using a climatological snow depth [Markus and Cavalieri, 1998] (MandC) or are – similar to OC2013 and KandM – trying to avoid utilizing snow depth information by using modified sea ice density values [Worby et al., 2008] (Worby). All these approaches are described in Section 3.1. We note that only for SICCI and OC2013 approaches we provide sea ice thickness uncertainties. We did not feel confident to i) estimate an uncertainty for the snow depth climatology or ii) for the modified sea ice density.

Figure 4.3 to Figure 4.5 give sample maps and corresponding histograms of the sea ice thickness distribution computed with the approaches mentioned before for period FM04 to ON04. Table 4.5 to Table 4.10 summarize the modal and mean sea ice thickness values computed for every ICESat-period listed in Table 2.1 for each of the approaches shown in Figures 4.3 to 4.5.

For FM04 (Figure 4.3; Table 4.5; Table 4.6), at first glance sea ice thickness maps and histograms for SICCI and OC2013AAall seem to be most similar to each other with the bulk of sea ice thickness values between 0 and 2 m. Also the corresponding uncertainty maps appear to be quite similar with uncertainties between 0 and 1 m. MandC sea ice thickness is similar to SICCI in the Ross and Amundsen Sea but shows considerably thicker sea ice in the Bellingshausen and southern and western parts of the Weddell Sea where sea ice thickness of or close to 4 m are observed. Worby sea ice thickness is less thick in these afore-mentioned regions: 2-3 m instead of 3-4 m. At the same time, however, the Worby sea ice thickness is larger in the Ross and northeastern Weddell Seas.

Tables 4.5 and 4.6 confirm the results shown in Figure 4.3. Indeed SICCI and OC2013AAall modal sea ice thickness agree closest with each other out of the 4 approaches shown in Figure 4.3: the all FM-period average is 0.90 m for SICCI and 0.84 m for OC2013AAall. The agreement in the mean sea ice thickness is less good with an all FM-period average of 1.60 m and 1.13 m for SICCI and OC2013AAall, respectively. The other empirical approaches based on OC2013: OC2013EA and OC2013WWS, also provide modal and mean sea ice thickness values close to SICCI for FM periods – particularly OC2013EA (see next subsection). MandC is identical to SICCI except that a climatological snow depth is used. While for FM periods the modal sea ice thickness is quite similar to SICCI (actually the second closest agreement of the all FM-period average) the mean sea ice thickness is the highest of the approaches considered: 2.01 m as the all FM-period averaged. Worby, finally, is similar to the case of $F < S$ of the SICCI approach, compare Equations (2) and (8); actual snow depth data are also not included. Out of the four compared approaches Worby sea ice thickness show by far the largest modal value: 1.39 m while the all FM-period average mean sea ice thickness is 1.86 m and hence between SICCI and MandC.

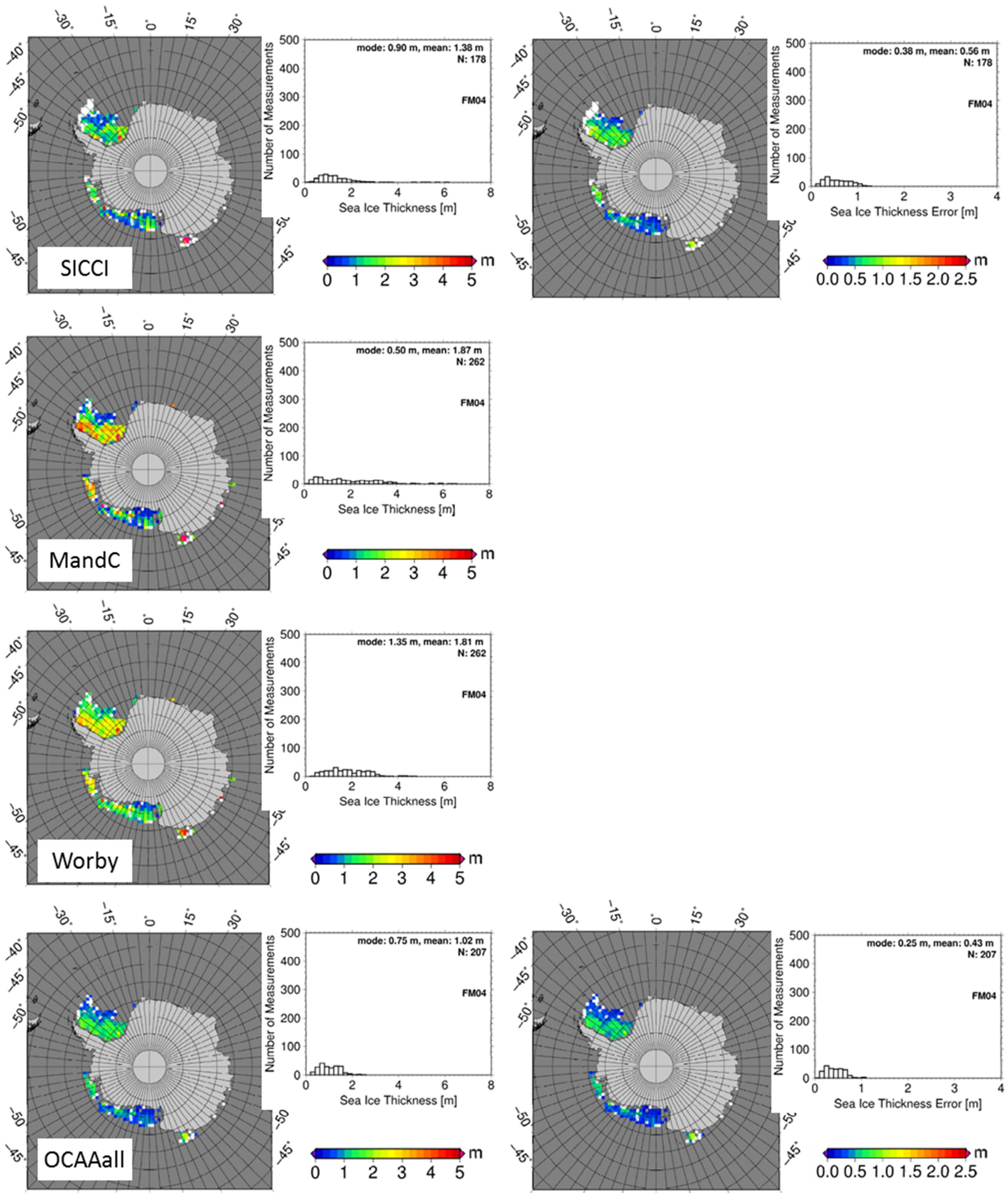

Figure 4.3: Sea ice thickness distribution around the Antarctic for – from top to bottom – SICCI, MandC, Worby, and OCAAall (left column) for FM04. White areas in the maps show grid cells with sea ice but without enough valid sea ice thickness data. Grid cell size is 100 km. Only grid cells with a sea ice concentration above 60% are shown. Each map is accompanied by a histogram showing the sea ice thickness distribution using bins of 0.2 m width. In each histogram the modal and mean sea ice thickness is given together with the number of valid data points N. The right columns displays maps of the respective sea ice thickness uncertainty for SICCI and OCAAall together with the corresponding histogram. Note that OCAAall and OC2013AAall refer to the same approach.

Table 4.5: Modal sea ice thickness from ICESat for FM periods from the SICCI algorithm in comparison to approaches MandC, Worby, OC2013AAall, OC2013EA, and OC2013WWS (see Section 3.1). The last column denotes the average value of the five FM periods. “Stdv” denotes one standard deviation of the values over the five FM periods.

Modal SIT, FM	2004	2005	2006	2007	2008	Mean ± Stdv
SICCI	0.90	1.10	0.70	0.90	0.90	0.90 ± 0.14
MandC	0.50	1.50	1.10	0.50	0.50	0.82 ± 0.46
Worby	1.35	1.50	1.30	0.90	1.90	1.39 ± 0.36
OC2013AAall	0.75	0.90	0.90	0.50	1.15	0.84 ± 0.24
OC2013EA	0.90	1.15	1.15	0.75	1.15	1.02 ± 0.19
OC2013WWS	0.70	0.75	0.90	0.50	0.90	0.75 ± 0.17

Table 4.6: As Table 4.5 but for the mean sea ice thickness for FM periods.

Mean SIT, FM	2004	2005	2006	2007	2008	Mean ± Stdv
SICCI	1.38	1.82	1.78	1.62	1.38	1.60 ± 0.21
MandC	1.87	2.44	2.25	1.65	1.85	2.01 ± 0.32
Worby	1.81	2.11	1.98	1.64	1.77	1.86 ± 0.18
OC2013AAall	1.02	1.20	1.09	1.38	0.95	1.13 ± 0.17
OC2013EA	1.30	1.52	1.38	1.75	1.20	1.43 ± 0.21
OC2013WWS	0.90	1.06	0.96	1.23	0.84	1.00 ± 0.15

Table 4.7: Modal sea ice thickness from ICESat for MJ periods from the SICCI algorithm in comparison to approaches MandC, Worby, OC2013AAall, OC2013EA, and OC2013WWS (see Section 3.1). The last column denotes the average value of the three MJ periods. “Stdv” denotes one standard deviation of the values over the three MJ periods.

Modal SIT, MJ	2004	2005	2006	Mean ± Stdv
SICCI	0.90	0.70	0.90	0.83 ± 0.12
MandC	0.90	1.10	1.15	1.05 ± 0.13
Worby	0.90	1.10	0.90	0.97 ± 0.12
OC2013AAall	0.70	0.75	0.70	0.72 ± 0.03
OC2013EA	0.90	0.90	0.90	0.90 ± 0.00
OC2013WWS	0.70	0.70	0.70	0.70 ± 0.00

Table 4.8: As Table 4.7 but for the mean sea ice thickness for MJ periods.

Mean SIT, MJ	2004	2005	2006	Mean ± Stdv
SICCI	1.21	1.41	1.38	1.33 ± 0.11
MandC	1.57	1.83	1.64	1.68 ± 0.13
Worby	1.32	1.45	1.34	1.37 ± 0.07
OC2013AAall	0.83	0.87	0.81	0.84 ± 0.03
OC2013EA	1.04	1.10	1.03	1.06 ± 0.04
OC2013WWS	0.74	0.78	0.73	0.75 ± 0.03

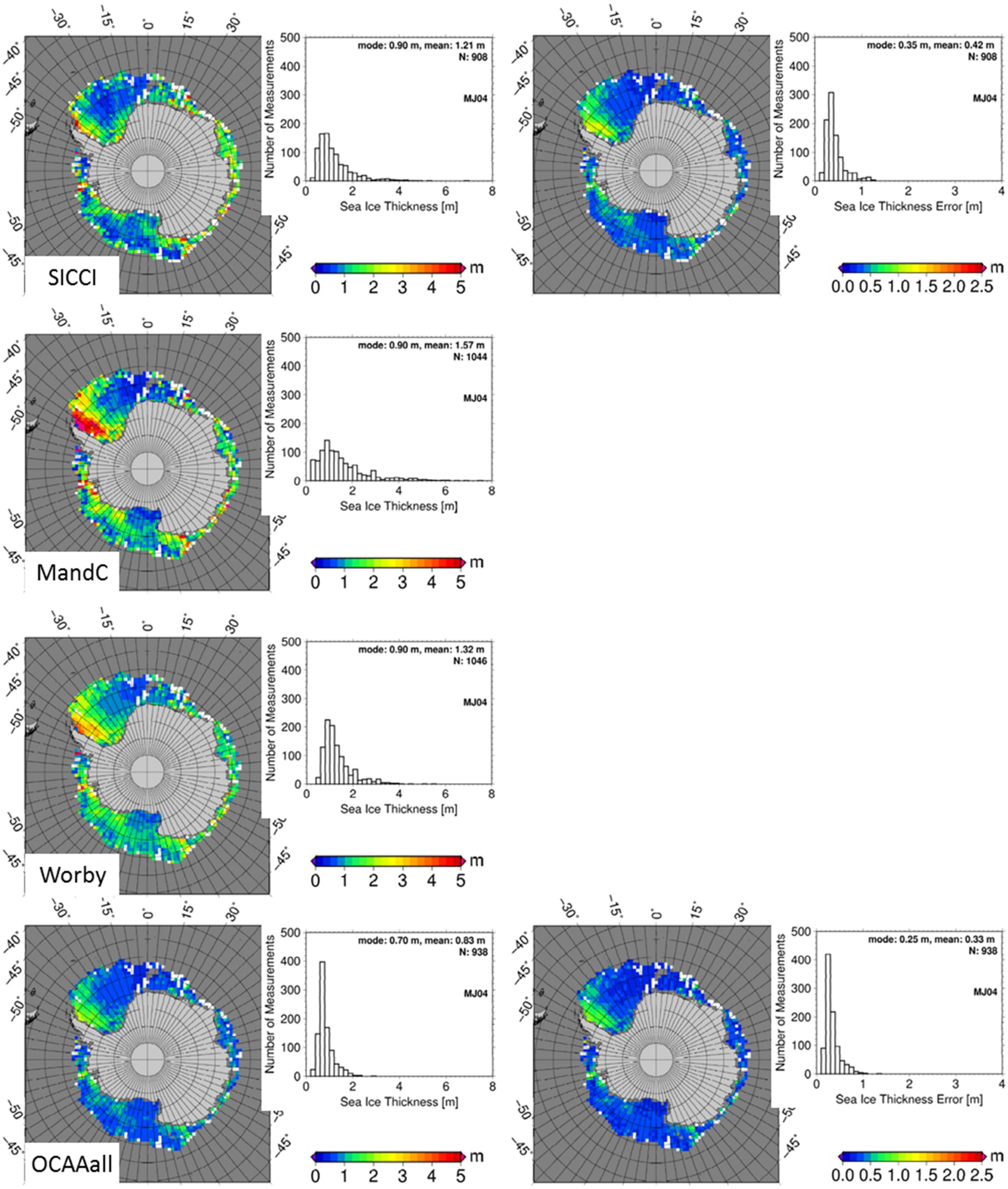

Figure 4.4: As Figure 4.3 but for ICESat period MJ04.

For period MJ04 (Figure 4.4, Table 4.7, Table 4.8) it becomes evident that SICCI and Worby are more similar in the spatial sea ice thickness distribution as well as in the sea ice thickness probability over the shown thickness range. The two respective maps and histograms are quite similar. SICCI has more thin ice in the Weddell and Ross/Amundsen Seas than Worby, though. Also the thickest ice to be found in the western Weddell Sea hugs the Antarctic Peninsula more closely than in Worby, where thicker ice extends a bit further to the East. Sea ice thickness in the Eastern Antarctic seems quite similar between the two approaches. This good agreement also occurs in years 2005 and 2006 so that the all MJ-period average mean sea ice thickness values agree within 0.05 m (Table 4.8).

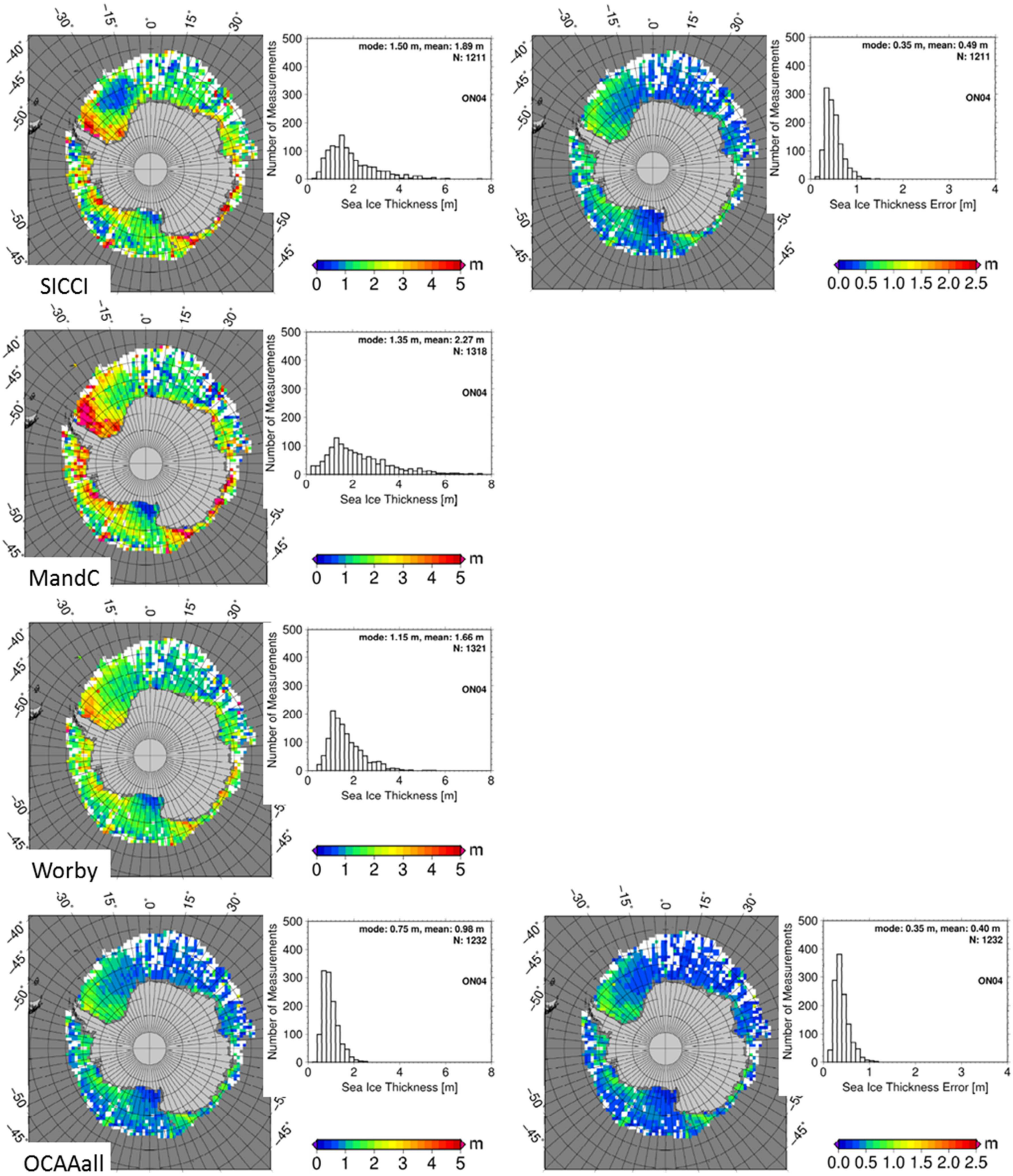

Figure 4.5: As Figure 4.3 but for ICESat period ON04.

For MandC sea ice thickness distribution is more similar to Worby than to SICCI (Figure 4.4, maps), however, the gradients are more pronounced. Where Worby shows thin ice MandC tends to show even thinner ice (Weddell and Ross Seas) and where Worby shows thick ice MandC shows even thicker ice. The latter applies especially to the western Weddell Sea where MandC shows a large area with sea ice thickness values above 4 m. While the MandC modal sea ice thickness is similar to SICCI and Worby the tails towards thicker ice is more pronounced and extends to larger thickness values. This seems also to be the case for the other two years because MandC shows the largest all MJ-period average mean sea ice thickness: 1.68 m of the 4 approaches compared in Figure 4.4. The all MJ-period average modal sea ice thickness is also the largest one of the 4 approaches but agrees with the Worby one within < 0.1 m.

OC2013AAall sea ice thickness shows a very pronounced peak at a modal value of 0.7 m and hence 0.2 m below the modal values of the other three approaches compared in Figure 4.4. Also there is almost no thick ice; the histogram quickly tails to zero at sea ice thickness values close to 2 m. This is the same for 2005 and 2006 (not shown) and consequently the all MJ-period average mean OC2013AAall sea ice thickness is the smallest of the four approaches: 0.84 m. This is almost half the value provided by Worby. In that respect OC2013AAall is quite similar to KandM (Figure 4.1, Tables 4.1 and 4.2) which revealed even smaller all MJ-period average modal and mean sea ice thickness values.

For period ON04 (Figure 4.5, Table 4.9, Table 4.10) the most pronounced change in the sea ice thickness distribution of all approaches is an increase in sea ice thickness and in the amount of thick ice. Modal and mean sea ice thickness values increase. The largest shifts in the histograms occur for SICCI and MandC. For all but OC2013AAall one can say that most regions showing sea ice thickness values between 0 and 1 m (1 and 2 m) in MJ (Figure 4.4) now show sea ice thickness values between 1 and 2 m(2 and 3 m) in ON (Figure 4.5). The number of grid cells with sea ice thicker than 3 m has also increased. Common to all approaches is the low sea ice thickness in the Ross Sea downstream of the Ross Ice Shelf polynya. The main difference between MandC and Worby is that MandC has by far more thick sea ice. The main difference between MandC and Worby on the one hand and SICCI on the other hand is the large region of sea ice thinner than 1 m in the central Weddell Sea.

Table 4.9: Modal sea ice thickness from ICESat for ON periods from the SICCI algorithm in comparison to approaches MandC, Worby, OC2013AAall, OC2013EA, and OC2013WWS (see Section 3.1). The last column denotes the average value of the four ON periods. "Stdv" denotes one standard deviation of the values over the four ON periods

Modal SIT, ON	2004	2005	2006	2007	Mean ± Stdv
SICCI	1.50	1.30	1.50	1.30	1.40 ± 0.12
MandC	1.35	1.10	1.30	1.35	1.28 ± 0.12
Worby	1.15	1.15	1.15	1.15	1.15 ± 0.00
OC2013AAall	0.75	0.75	0.75	0.90	0.79 ± 0.08
OC2013EA	0.90	0.90	0.90	1.10	0.95 ± 0.10
OC2013WWS	0.70	0.70	0.70	0.75	0.71 ± 0.03

Table 4.10: As Table 4.9 but for the mean sea ice thickness for ON periods.

Mean SIT, ON	2004	2005	2006	2007	Mean ± Stdv
SICCI	1.89	1.84	1.94	1.78	1.86 ± 0.07
MandC	2.27	2.08	2.25	2.11	2.18 ± 0.10
Worby	1.66	1.55	1.63	1.57	1.60 ± 0.05
OC2013AAall	0.98	0.92	0.96	0.95	0.95 ± 0.03
OC2013EA	1.24	1.17	1.21	1.20	1.21 ± 0.03
OC2013WWS	0.87	0.82	0.85	0.84	0.85 ± 0.02

The sea ice thickness increase provided by OC2013AAall is far less pronounced; the increase in the modal sea ice thickness from MJ04 to ON04 is 0.05 m, the corresponding increase in mean sea ice thickness is 0.13 m. Note that KandM modal (mean) sea ice thickness change from MJ04 to ON04 was -0.05 m and 0.10 m. Sea ice thickness values above 2 m are almost absent in the OC2013AAall product – also similar to KandM (Figure 4.1, Tables 4.1 and 4.2).

For ON periods, in contrast to FM and MJ, the largest modal sea ice thickness values are provided by SICCI, followed by MandC, Worby, and OC2013AAall in descending order. With regard to the mean sea ice thickness, MandC and SICCI switch places in the order but still SICCI provides a quite high mean sea ice thickness: 1.89 m compared to 2.27 m (MandC) and 1.66 m (Worby). When considering all ON periods this ranking stays. SICCI provides the highest all ON-period average modal sea ice thickness: 1.40 m (followed by MandC) and the second-highest all ON-period average mean sea ice thickness: 1.86 m (preceded by MandC).

Table 4.11 provides an overview about the all FM-, MJ-, and ON-period average modal and mean sea ice thickness values of all approaches considered in Figures 4.3 to 4.5, the two addition OC2013 approaches (see next subsection) and the KandM approach.

The average mean sea ice thickness decreases from FM to MJ for all approaches. This can be explained by the fact that most of the sea ice during FM is perennial ice which is hence thicker, on average, than the mean sea ice thickness in MJ when the ice cover still contains most of this perennial ice, which presumably has also already thickened quite a bit, but when the bulk of the ice cover comprises newly grown seasonal sea ice. If we look at the change in the average mean sea ice thickness from MJ to ON then we have two classes of approaches. One class shows a substantial increase in sea ice thickness: 0.53 m (SICCI), 0.50 m (KandM), and 0.37 m (Worby). The other class shows a small increase in sea ice thickness: 0.04 m (KandM), 0.11 m (OC2013AAall), 0.15 m (OC2013EA), and 0.10 m (OC2013WWS).

Table 4.11: Summary of the average modal (normal font) and mean (bold font) sea ice thickness for each seasonal period, i.e. for FM, MJ, and ON, for all approaches used with ICESat data. The second value in each cell is one standard deviation of the average over the 5, 3, and 4 periods, respectively.

Method	SICCI	KandM	MandC	Worby	AAall	EA	WWS
FM, mode	0.90±0.14	0.85±0.16	0.82±0.46	1.35±0.43	0.84±0.24	1.02±0.19	0.75±0.17
FM, mean	**1.61±0.21**	**0.82±0.15**	**2.01±0.32**	**1.98±0.20**	**1.13±0.17**	**1.43±0.21**	**1.00±0.15**
MJ, mode	0.83±0.12	0.43±0.12	1.05±0.13	0.97±0.12	0.72±0.03	0.90±0.00	0.70±0.00
MJ, mean	**1.33±0.11**	**0.63±0.05**	**1.68±0.13**	**1.37±0.07**	**0.84±0.03**	**1.06±0.04**	**0.75±0.03**
ON, mode	1.40±0.12	0.43±0.09	1.28±0.12	1.15±0.00	0.79±0.08	0.95±0.10	0.71±0.03
ON, mean	**1.86±0.07**	**0.67±0.05**	**2.18±0.10**	**1.60±0.05**	**0.95±0.03**	**1.21±0.03**	**0.85±0.02**

The average modal sea ice thickness decreases from FM to MJ for all approaches but MandC. Given the fact that modal values might be difficult to find for the more data sparse FM periods this outlier for MandC should not be over-interpreted. The observed decrease is however what we'd expect for the same reason as we expect a decrease in the mean sea ice thickness from FM to MJ. For the change in average modal sea ice thickness from MJ to ON we can again identify two classes. For one class we observe a pronounced increase in modal sea ice thickness: 0.57 m (SICCI), 0.23 m (MandC), and 0.18 m (Worby). For the other class we either see (almost) no change: 0.00 m (KandM), 0.01 m (OC2013WWS) or just a small increase: 0.07 m (OC2013AAall) and 0.05 m (OC2013EA). This will also be discussed in subsection 4.4.

The sea ice thickness uncertainty maps and corresponding histograms shown in Figures 4.3 to 4.5, right column, reveal the following main issues: i) the input parameters allow a reasonable derivation of the uncertainty for every grid cell; ii) modal and mean sea ice thickness uncertainties stay within reasonable bounds and reveal modal values between 0.3 and 0.5 m and mean values which are slightly larger; iii) sea ice thickness uncertainty levels off at values around 1 m; iv) largest sea ice thickness uncertainties occur in areas of largest sea ice thickness and hence presumably also deepest snow. This seems logical because the main contributor to the sea ice thickness uncertainty is the snow depth uncertainty which is set to 0.3 times snow depth and also freeboard or freeboard and snow depth enter the uncertainty computation (see Equations (3), (4), and (6)).

Table 4.12 and Table 4.13 summarize the sea ice thickness uncertainties as all FM-, MJ-, and On-period average modal (Table 4.12) and mean (Table 4.13) values for SICCI and OC2013AAall. Largest modal values occur for FM: 0.45 m (SICCI) and 0.34 m (OC2013AAall) while the smallest occur for MJ: 0.32 m (SICCI) and 0.24 m (OC2013AAall). The same can be observed for the mean values which are about 0.1 m higher than the modal values.

Table 4.12: Modal value of the sea ice thickness retrieval uncertainty averaged over the 5, 3 and 4 ICESat periods in FM, MJ, and ON, respectively, for SICCI and OC2013AAall. The second value in every cell is the standard deviation of the modal values over the periods

ICESat period	FM	MJ	ON
SICCI	0.45 ± 0.16	0.32 ± 0.06	0.37 ± 0.01
OC2013AAall	0.34 ± 0.05	0.24 ± 0.01	0.33 ± 0.05

Table 4.13: As Table 4.12 but for the mean sea ice thickness retrieval uncertainty.

ICESat period	FM	MJ	ON
SICCI	0.55 ± 0.05	0.41 ± 0.02	0.49 ± 0.07
OC2013AAall	0.47 ± 0.07	0.33 ± 0.02	0.39 ± 0.01

4.1.3 OC2013 approach inter-comparison

The empirical approaches developed by Ozsoy-Cicek et al. [2013] offer various possibilities to compute sea ice thickness from total freeboard. Linear regression coefficients are derived for five different regions. In the current work we averaged the coefficients of these regions to end up with a set of coefficients we think is valid for the entire Antarctic. This is the one termed OC2013AAall. Here we compare sea ice thickness obtained with that approach with two of those originally published for East Antarctica (OC2013EA) and the Western Weddell Sea (OC2013WWS) (Section 3.1).

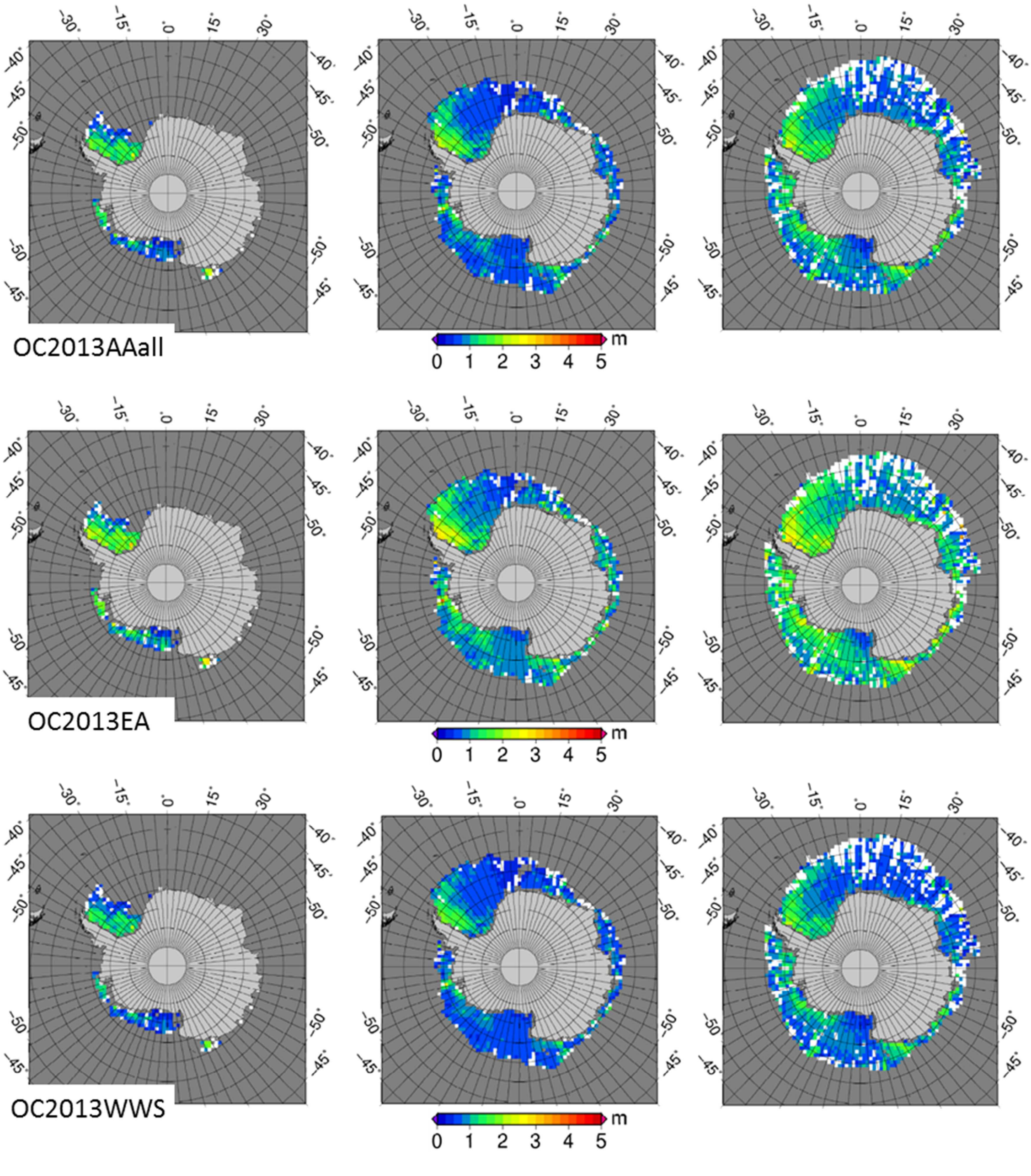

Figure 4.6: Sea ice thickness distribution around the Antarctic for – from top to bottom – OC2013AAall, OC2013EA, and OC2013WWS for – from left to right – FM04, MJ04, and ON04. White areas in the maps show grid cells with sea ice but without enough valid sea ice thickness data. Grid cell size is 100 km. Only grid cells with a sea ice concentration above 60% are shown.

Figure 4.6 shows the sea ice distribution maps obtained with the three selected OC2013 approaches for the ICESat periods in 2004. This figure illustrates that apparently the OC2013AAall and the OC2013WWS approach reveal quite similar results in terms of the absolute sea ice thickness values and in terms of the distribution while the OC2013EA approach provides substantially thicker sea ice. This is not only illustrated in Figure 4.6 but also in the Tables 4.5 to 4.10 and, in summary, in Table 4.11, and in Figure 4.7 below.

OC2013EA stands out for all ICESat periods listed in Table 2.1 as the OC2013 approach which provides the largest modal and largest mean sea ice thickness values for almost every period. The average modal sea ice thickness values computed with OC2013EA exceed those of the other two OC2013 approaches by 0.2 m for all seasons considered. The respective mean values exceed the others by 0.2 m to 0.4 m.

OC2013EA is also the only one of the three approaches which provides a considerable fraction of sea ice thickness values exceeding 2 m. However, still values up to 3 m or even 4 m as provided by SICCI, MandC, or Worby cannot be found in the results of the OC2013 approaches.

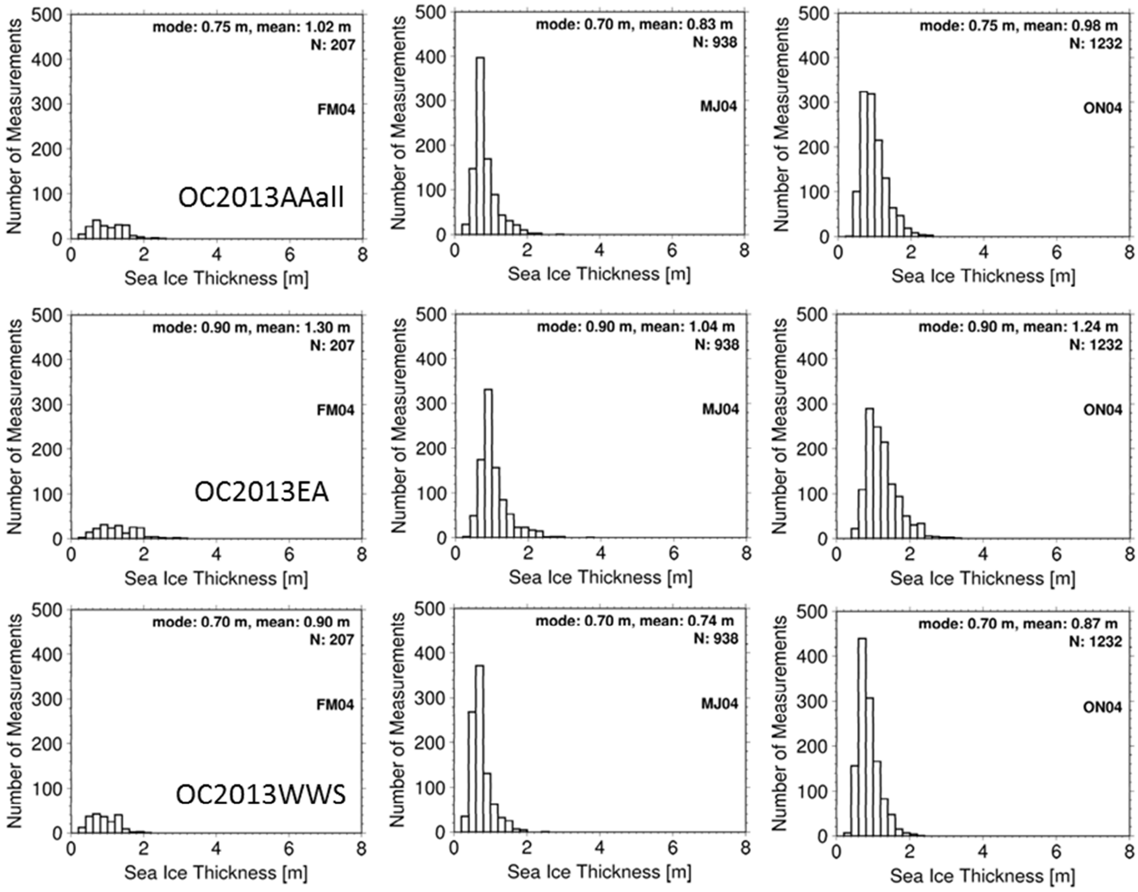

Figure 4.7: Histograms of the sea ice thickness corresponding to Figure 4.6. In each histogram the modal and mean sea ice thickness is given together with the number of valid data points N. Bin size is 0.2 m.

What is the difference between the three OC2013 approaches and which one is re-commended for the comparison with the other ICESat approaches? First of all, all three OC2013 approaches provide sea ice thickness values which are relatively similar to each other and also to KandM. This latter approach will be discussed in Subsection 4.4.4 The OC2013EA provides largest sea ice thickness values because it has the largest slope of the three OC2013 approaches considered (see Table 3.1). It also has the largest intercept of 0.26 m. In contrast OC2013WWS has the smallest slope of the three (Table 3.1) and a smaller intercept (0.22 m) so that it is not surprising that with this OC2013 approach (OC2013WWS) we compute the smallest sea ice thickness values. However, the question is how representative are these two sets of linear regression coefficients – generated from local measurements – in comparison to the circum-Antarctic average of the regression results? We think that it makes more sense to use an approach with a wider applicability – at least theoretically – than an approach which is based on a few local to regional measurements. Therefore we recommend and have also used already the OC2013AAall approach.

The sea ice thickness maps generated with OC2013EA and OC2013WWS shown in Figure 4.6 might reveal particularly realistic sea ice thickness values in those regions from which the data used to generate the linear relationship have been collected. If this would be true, then one would expect that the sea ice thickness obtained for the Western Weddell Sea with OC2013WWS does resemble the thickness which is typically measured there. This seems however not to be the case because even though sea ice thickness values are higher close to the Antarctic Peninsula than further East the values are far below those known from other studies involving ICESat data [Zwally et al., 2008; Yi et al., 2011; Kern and Spreen, 2015] and those known from in-situ observations [C. Haas, personal communication] or those to be expected from air-borne freeboard measurements [Kwok and Maksym, 2014]. For the region East Antarctic it is difficult to make a conclusion here due to the lack of data for inter-comparison. One could think, however, that sea ice thickness values in the range 1 to 2 m for most of the East Antarctic area in ON are more reasonable than the values between 2 and 4 m as suggested by SICCI or MandC (Figure 4.5). We note that for the East Antarctic region the approaches Worby (Figure 4.5) and OC2013EA (Figure 4.6) show quite similar results for ON.

4.2 Comparison ICESat-1 to Envisat RA2

This section compares sea ice thickness obtained from ICESat freeboard data using the SICCI approach with sea ice thickness obtained from contemporary Envisat RA2 data using the equations given in Section 3.2. Note that we follow a two-way approach and compute the sea ice thickness from Envisat RA2 assuming on the one hand that the radar freeboard represents the sea ice freeboard and that, on the other hand, the radar freeboard represents the total freeboard. Those values obtained for the case "radar freeboard = sea ice freeboard" are denoted with "sea ice F" or "IceFB". Those values obtained for the case "radar freeboard = total freeboard" are denoted with "total F" or "TotalFB".

Figure 4.8 to Figure 4.10 show maps of the sea ice thickness distribution for ICESat periods FM04, MJ04 and ON04 together with the respective histograms.

For period FM04 ICESat and Envisat RA2 sea ice thickness maps and histograms do not have too much in common. RA2 total F under-estimates the sea ice thickness compared to ICESat basically everywhere. The modal sea ice thickness value from RA2 total F is about 0.4 m below the one of ICESat and the mean sea ice thickness is about half the ICESat value. In contrast, RA2 sea ice F over-estimates ICESat sea ice thickness also basically everywhere. The modal sea ice thickness value is 3.25 m, the mean value is 2.64 m, both much higher than the respective ICESat values.

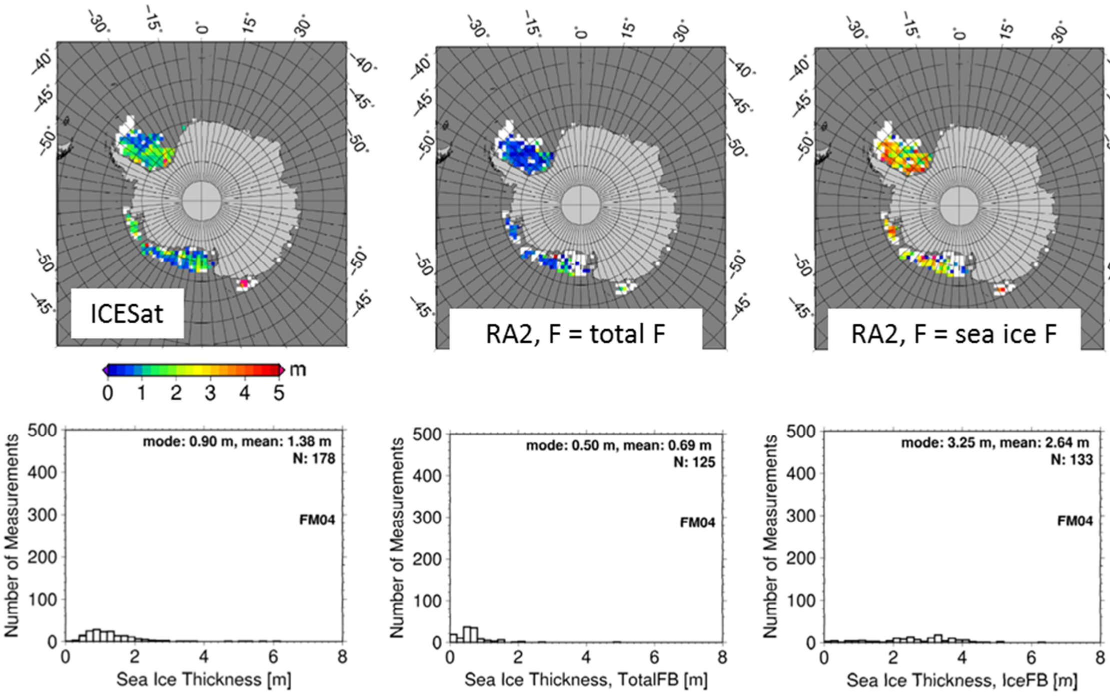

Figure 4.8: Sea ice thickness distribution around the Antarctic for – from left to right – ICESat SICCI, Envisat RA2 total F, and Envisat RA2 sea ice F for ICESat period FM04. White areas in the maps show grid cells with sea ice but without enough valid sea ice thickness data. Grid cell size is 100 km. Only grid cells with a sea ice concentration above 60% are shown. Each map is accompanied by a histogram showing the sea ice thickness distribution using bins of 0.2 m width. In each histogram the modal and mean sea ice thickness is given together with the number of valid data points N. Note that for each product all valid points are shown and used in order to keep the amount of values at a reasonable level.

Table 4.14: Modal sea ice thickness for ICESat period FM in comparison to the modal sea ice thickness from Envisat RA2 for case "Total F" and for case "sea ice F". The last column gives the all FM-period average plus/minus one standard deviation.

Year	2004	2005	2006	2007	2008	Mean ± Stdv
ICESat	0.90	1.10	0.70	0.90	0.90	0.90 ± 0.14
RA2, total F	0.50	0.50	0.45	0.45	0.50	0.48 ± 0.03
RA2, sea ice F	3.25	2.30	2.65	2.35	2.25	2.56 ± 0.42

Table 4.15: As Table 4.14 but for the mean sea ice thickness of period FM.

Year	2004	2005	2006	2007	2008	Mean ± Stdv
ICESat	1.38	1.82	1.78	1.62	1.38	1.60 ± 0.21
RA2, total F	0.69	0.88	0.94	1.11	0.89	0.90 ± 0.15
RA2, sea ice F	2.64	2.96	2.66	2.55	2.62	2.69 ± 0.16

Tables 4.14 and 4.15 reveal that this pattern: under-estimation of ICESat sea ice thickness by RA2 total F and over-estimation of ICESat sea ice thickness by RA2 sea ice F is valid for all FM periods. On average, modal values are 0.90 m (SICCI), 0.48 m (RA total F), and 2.56 m (RA sea ice F)

(Table 4.14) and mean values are 1.60 m (SICCI), 0.90 m (RA total F), and 2.69 m (RA sea ice F) (Table 4.15).

Therefore, during FM periods assuming that the radar senses the sea ice freeboard results in an over-estimation of the all FM-period average mean ICESat SICCI sea ice thickness of about 1.1 m. In contrast assuming that the radar senses the total freeboard results in an under-estimation of the same thickness value by about 0.7 m. Note that the all FM-period average mean sea ice thickness computed with RA2 sea ice F does, however, agree with the respective ICESat KandM value (Table 4.11).

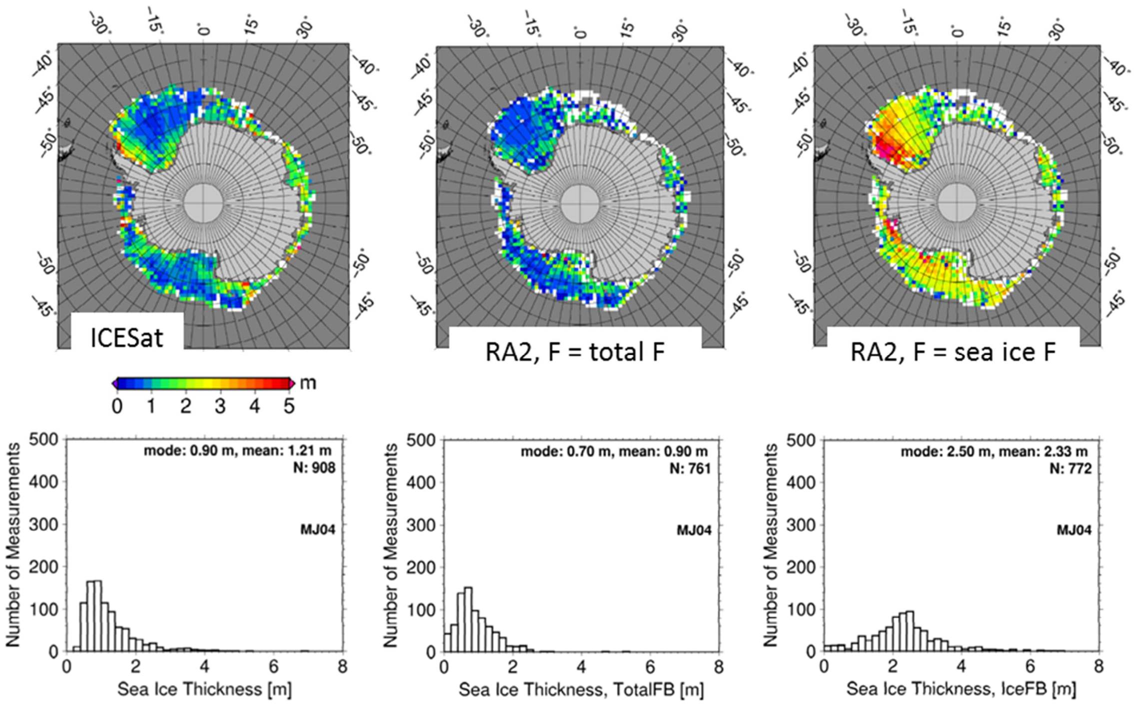

Figure 4.9: As Figure 4.8 but for ICESat period MJ04.

For ICESat period MJ04 (Figure 4.9) the sea ice thickness distributions of ICESat SICCI and RA2 agree much better with each other than for FM04 (Figure 4.8). Sea ice thickness from RA2 total F agrees in fact quite well with ICESat sea ice thickness except for the region east of the Antarctic Peninsula where RA2 total F lacks the thicker sea ice common here. Accordingly the histograms look quite similar as well and the modal and mean sea ice thickness values agree closer with each other than for FM; the modal values are 0.9 m and 0.7 m for ICESat and RA2 total F, respectively, and the mean values are 1.21 m and 0.90 m. RA2 total F tends to show more thin ice with close to 50 counts in the bins 0 – 0.2 m and 0.2 to 0.4 m while ICESat has no counts in bin 0 to 0.2 m and perhaps 10 counts in the other bin. Sea ice thickness computed with RA sea ice F has some similarity to ICESat but not so much to RA total F sea ice thickness. The sea ice thickness obtained with RA sea ice F has high values, i.e. > 3 m, in those regions where perennial ice can be expected, i.e. in parts of the southeastern Ross Sea, southern Amundsen Sea and western Weddell Sea. The extent of the thick ice in the latter region is, however, much wider than for ICESat. Not too many sea ice thickness values < 1 m can be found – which is also visible in the corresponding histogram; actually only about 50 of the 772 valid value have a sea ice thickness < 1 m. Accordingly, the modal and the mean sea ice thickness provided by RA2 sea ice F are much higher than ICESat SICCI and RA2 total F: 2.50 m and 2.33 m.

Table 4.16: Modal sea ice thickness for ICESat period MJ in comparison to the modal sea ice thickness from Envisat RA2 for case "Total F" and for case "sea ice F". The last column gives the all MJ-period average value plus / minus one standard deviation.

Year	2004	2005	2006	Mean ± Stdv
ICESat	0.90	0.70	0.90	0.83 ± 0.12
RA2, total F	0.70	0.50	0.45	0.55 ± 0.13
RA2, sea ice F	2.50	2.10	1.95	2.18 ± 0.28

Table 4.17: As Table 4.16 but for the mean sea ice thickness of period MJ.

Year	2004	2005	2006	Mean ± Stdv
ICESat	1.21	1.41	1.38	1.33 ± 0.11
RA2, total F	0.90	0.95	0.96	0.94 ± 0.03
RA2, sea ice F	2.33	2.30	2.13	2.25 ± 0.11

Tables 4.16 and 4.17 confirm that similar to the FM periods, the impression given by the example from 2004, MJ04, is valid for the other two MJ periods as well. Lowest all MJ-period average modal and mean sea ice thickness values are provided with RA2 total F: 0.55 m and 0.94 m, respectively, values which are 0.3 m and 0.4 m below those for ICESat, whereas RA2 sea ice F provides all MJ-period average modal and mean sea ice thickness values of 2.18 m and 2.25 m, respectively.

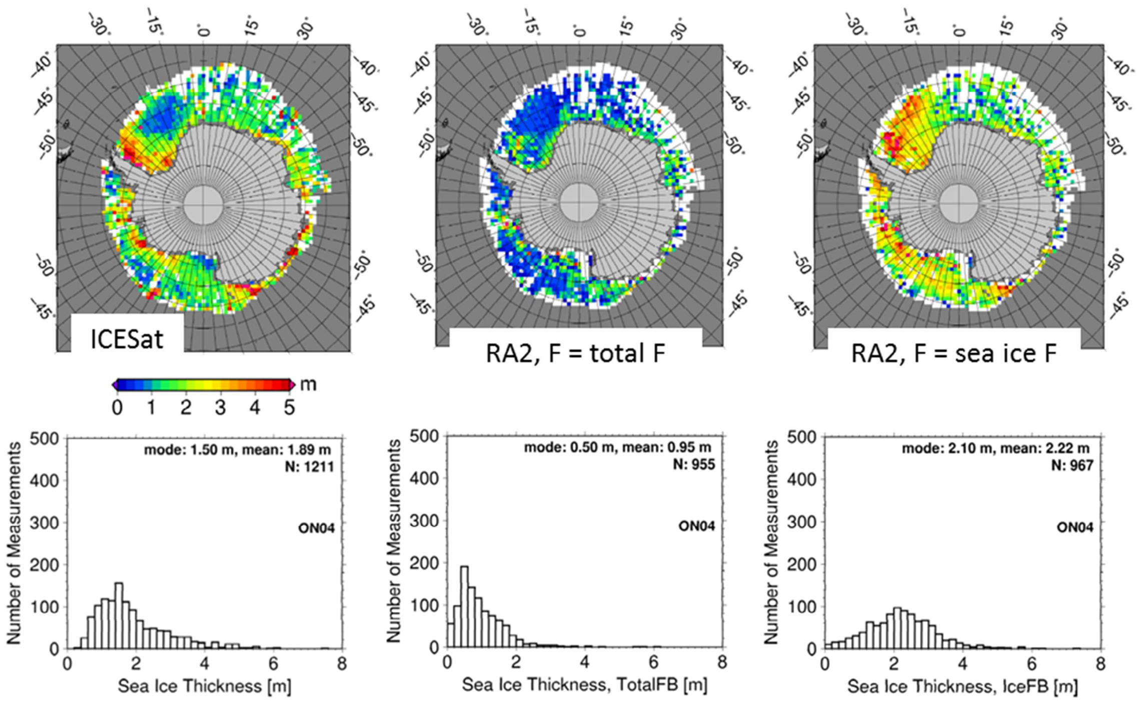

Figure 4.10: As Figure 4.8 but for ICESat period ON04.

Table 4.18: Modal sea ice thickness for ICESat period ON in comparison to the modal sea ice thickness from Envisat RA2 for case "Total F" and for case "sea ice F". The last column gives the all ON-period average modal value plus / minus one standard deviation.

Year	2004	2005	2006	2007	Mean ± Stdv
ICESat	1.50	1.30	1.50	1.30	1.40 ± 0.12
RA2, total F	0.50	0.30	0.45	0.45	0.43 ± 0.09
RA2, sea ice F	2.10	1.90	1.90	2.10	2.00 ± 0.12

Table 4.19: As Table 4.18 but for the mean sea ice thickness for ON periods.

Year	2004	2005	2006	2007	Mean ± Stdv
ICESat	1.89	1.84	1.94	1.78	1.86 ± 0.07
RA2, total F	0.95	0.90	0.91	0.84	0.90 ± 0.05
RA2, sea ice F	2.22	1.92	1.99	2.06	2.05 ± 0.13

Figure 4.10 gives the impression that now the RA2 sea ice F sea ice thickness distribution agrees more closely with ICESat SICCI than RA2 total F. However, this has less to do with changes in the sea ice thickness in the RA2 maps but more with the changes between MJ04 and ON04 in the ICESat map. This is confirmed by the corresponding histograms. For RA2 their shape did not too much and surprisingly the modal sea ice thickness decreases from MJ04 to ON04 by 0.2 m from 0.7 m to 0.5 m for RA2 total F and by 0.4 m from 2.5 m to 2.1 m for RA2 sea ice F. For the latter also the mean sea ice thickness decreased from 2.33 m to 2.22 m. This contradicts the development shown by ICESat SICCI: an increase in modal and mean sea ice thickness by 0.6 m from MJ04 to ON04. Note that the general distribution of the thickest ice is similar between ICESat and RA2 sea ice F – except in the north-western Weddell Sea where these two approaches show the largest discrepancy.

Tables 4.18 and 4.19 again confirm that 2004 seems to be quite typical for the 4 ON periods considered. RA2 total F provided the lowest all ON-period average modal: 0.43 m and mean: 0.90 m sea ice thickness values – in agreement with ICESat KandM (Table 4.11). ICESat SICCI provided much larger values: 1.40 m and 1.86 m which are, however, much closer to those provided by RA2 sea ice F: 2.00 m and 2.05 m, respectively, than for FM and MJ periods. There are in fact larger regions where the sea ice thickness distribution from ICESat SICCI and RA2 sea ice F are almost identical.

This change in agreement between ICESat and the two RA2 approaches from FM over MJ to ON periods in total sea ice thickness values on the one hand and the spatial sea ice thickness distribution on the other hand will be illustrated further down in Figure 4.11.

Beforehand we note upon the sea ice thickness retrieval uncertainties. These are computed using the respective equations given in Section 3.1 and 3.2 and are summarized in Tables 4.20 and 4.21 as the all FM-, MJ-, and ON-period average modal and the mean sea ice thickness uncertainties.

The average modal uncertainties for RA2 are higher than those for ICESat (Table 4.20) which vary between 0.32 m (MJ) and 0.45 m (FM). RA2 sea ice F exceeds the values for ICESat SICCI by 0.25 m for FM and MJ and by 0.17 m for ON. RA2 total F exceeds the values for ICESat SICCI by between 0.06 m (FM) and 0.16 m (MJ).

Table 4.20: Modal value of the sea ice thickness retrieval uncertainty averaged over the 5, 3, and 4 ICESat periods in FM, MJ, and ON. The second value is the standard deviation of the modal values over the periods.

ICESat period	FM	MJ	ON
ICESat	0.45 ± 0.16	0.32 ± 0.06	0.37 ± 0.01
RA2, total F	0.51 ± 0.05	0.48 ± 0.06	0.48 ± 0.05
RA2, sea ice F	0.70 ± 0.15	0.57 ± 0.02	0.54 ± 0.06

The average mean uncertainties are higher than the modal ones for ICESat SICCI but not for RA2 – which could simply be caused by the fact that we chose the RA2 freeboard uncertainty dF as fraction of F while for ICESat dF is actually computed from the data. RA2 total F sea ice thickness uncertainties are around those for ICESat while those of RA2 sea ice F still exceed those of the other two approaches be between 0.1 m and 0.2 m.

Table 4.21: As Table 4.20 but for mean value of the sea ice thickness retrieval uncertainty.

ICESat period	FM	MJ	ON
ICESat	0.55 ± 0.05	0.41 ± 0.02	0.48 ± 0.01
RA2, total F	0.53 ± 0.03	0.49 ± 0.02	0.44 ± 0.03
RA2, sea ice F	0.71 ± 0.04	0.58 ± 0.03	0.53 ± 0.03

We note that even though the RA2 total F sea ice thickness uncertainty is smaller than the one for RA2 sea ice F the relative uncertainty is much larger for this approach. Why is this? RA2 sea ice F provides modal and mean sea ice thickness values between 2 m and 3 m and hence an uncertainty of 0.5 to 0.7 m corresponds to a relative error of between 15 % and 33%. In contrast, RA2 total F provides modal and mean sea ice thickness values between 0.4 m and 0.9 m and hence an uncertainty of 0.4 to 0.5 m corresponds to a relative error of between 45% and 120%.

Now that we know that the average sea ice thickness uncertainty is around 0.4 to 0.5 m it makes sense to take a look at the differences to reveal where – locally – ICESat and RA2 agree most. For this purpose we computed the difference ICESat SICCI sea ice thickness minus RA2 sea ice thickness for every grid cell separately for both RA2 approaches. Similarly to the plain sea ice thickness results we generated histograms of the sea ice thickness differences and derived the modal and mean sea ice thickness differences. The difference maps and corresponding histograms are shown in Figure 4.11 for ICESat periods in 2004. The all FM-, MJ-, ON-period average modal and mean sea ice thickness differences are summarized in Table 4.22.

For FM04 (Figure 4.11, top row) the Weddell Sea is the area where ICESat SICCI predominantly over-estimates RA2 total F sea ice thickness while it predominantly under-estimates RA2 sea ice F sea ice thickness. The small ice covered area and low number of valid data points makes further considerations difficult. The histograms confirm the impression: modal and mean sea ice thickness differences are 0.38 m and 0.83 m for RA2 total F and -1.6 m and -1.0 m for RA2 sea ice F.

For MJ04 (Figure 4.11, middle row) the good agreement between RA2 total F and ICESat SICCI is confirmed. Large areas have differences between -0.4 and 0.4 m, the distribution of differences around the modal value close to zero: 0.08 m is almost symmetrical with a mean difference of 0.32 m which lies within the average sea ice thickness uncertainty of both products. Note however, that large positive differences (under-estimation of ICESat SICCI by RA2) occur in particular in the southern, western, and north-western Weddell Sea regions which are known to be influenced by perennial ice. Larger positive differences do occur also along East Antarctica, in the southern Amundsen Sea, and also in the northern Ross and Amundsen Seas along the marginal ice zone.

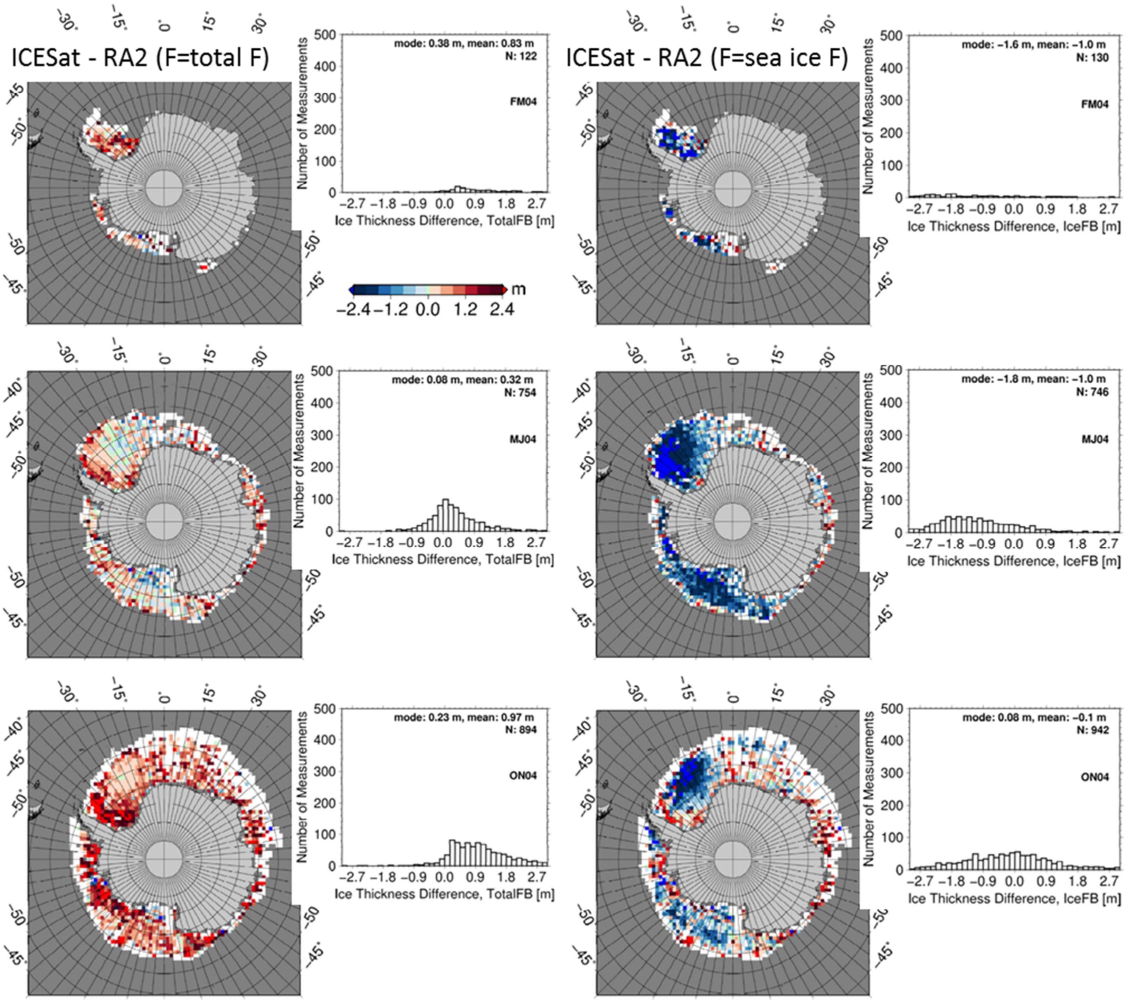

Figure 4.11: Difference in sea ice thickness ICESat minus RA2 for RA2 total F (left column) and RA2 sea ice F (right column) for ICESat periods – from top to bottom: FM04, MJ04, and ON04. White areas in the maps show grid cells with sea ice but without enough valid sea ice thickness data. Grid cell size is 100 km. Only grid cells with a sea ice concentration above 60% are shown. Each map is accompanied by a histogram showing the sea ice thickness difference distribution using bins of 0.15 m width. In each histogram the modal and mean sea ice thickness difference is given together with the number of valid data points N.

Figure 4.11, middle row, also confirms the substantial under-estimation of RA2 sea ice F sea ice thickness by ICESat SICCI. The difference map is dominated by large negative differences in the entire western Antarctic sea ice cover with the largest negative differences of more than 2 m occurring in the central Weddell Sea and in the Ross Sea. In the East Antarctic sea ice cover differences are smaller and there are quite some grid cells where ICESat SICCI over-estimates RA2 sea ice F sea ice thickness. Such an over-estimation is also observed along the ice edge, e.g. in the northern Ross Sea. These grid cells with RA2 sea ice F sea ice thickness over-estimation by ICESat SICCI are the main reason for the mean difference staying at a moderate -1.0 m while the modal difference takes a value of -1.8 m.

We note that many of those grid cells where ICESat SICCI sea ice thickness over-estimates RA2 sea ice F can be identified in the map of the sea ice thickness difference ICESat SICCI minus RA2 total F as well. This could point to grid cells where ICESat SICCI provides particularly invalid values. Some of these are actually quite likely artefacts as, e.g. the group of differences close to +2.0 m along 20°E (Figure 4.11, middle row). There is another patch of similarly high differences visible for ON04 in the Ross Sea at 150°W.

For ON04 (Figure 4.11, bottom row) it seems as if RA2 total F and RA2 sea ice F switch places – in agreement with our discussion of Figures 4.9 and 4.10. Now the difference ICESat SICCI minus RA2 sea ice F had a modal value close to zero: 0.08 m and tends to be almost symmetrical around this modal value with a mean difference of only -0.1 m. There are some regions, e.g. the Eastern Weddell Sea and parts of the Ross Sea, where the difference is between -0.4 m and 0.4 m. Still there are also two regions where the difference between ICESat SICCI and RA2 sea ice F is quite negative with values below -1.2 m or even below -2 m. These occur in the central Ross and Amundsen Seas and in the central Weddell Sea; especially the latter region takes attention because of sea ice thickness values below about 1 m in ON04 period (Figure 4.8, left).

These area, where RA2 sea ice F strongly under-estimates ICESat SICCI are exactly those areas where RA2 total F and ICESat SICCI agree best for ON04 period. These areas are responsible for the low modal value of 0.23 m which otherwise would be located at around 1 m (see respective histogram in Figure 4.11 bottom row). For almost the entire remaining sea ice cover RA2 total F under-estimates ICESat SICCI by at least 1 m, at many places by more than 2 m. Consequently the mean difference is 0.97 m.

Table 4.22: Modal and mean value of the difference ICESat sea ice thickness minus Envisat RA2 sea ice thickness averaged over the 5, 3, and 4 ICESat periods in FM, MJ, and ON. The second value in every cell is the standard deviation of the modal and mean values over the periods. Smallest differences are highlighted in bold font.

ICESat period		FM	MJ	ON
Modal SIT	ICESat-RA2, total F	**0.36 ± 0.07**	**0.13 ± 0.09**	0.72 ± 0.43
	ICESat-RA2, sea ice F	-1.68 ± 0.48	-1.37 ± 0.45	**0.05 ± 0.29**
Mean SIT	ICESat-RA2, total F	**0.74 ± 0.16**	**0.39 ± 0.06**	1.03 ± 0.06
	ICESat-RA2, sea ice F	**-0.74 ± 0.18**	-0.80 ± 0.20	**0.02 ± 0.13**

Table 4.22 illustrates nicely the switch between MJ periods and ON periods. While for MJ periods modal and mean sea ice thickness differences are smaller for RA2 total F, for ON periods these values are smaller for RA2 sea ice F. This will be discussed further in Section 4.4.

4.3 Comparison Envisat RA2 to CryoSat-2

After the failure of the Envisat satellite CryoSat-2 remains currently the main satellite to provide sea ice thickness information in Polar Regions. Here we compare the sea ice thickness distribution computed from Envisat-RA2 and CryoSat-2 for months January to September 2011. Similarly to what has been done in the previous subsection sea ice thickness is computed from the radar freeboard data in two ways. One assumes radar freeboard represents the total freeboard like measured by ICESat (denoted "total F" and "TotalFB"). The other assumes radar freeboard represents the sea ice freeboard like it should theoretically be the case for dry snow (denoted "sea ice F" and "IceFB"). The corresponding equations and description of input data are given in Section 3.2.

We first show sea ice thickness maps and corresponding histograms for months May and June in Figures 4.12 and 4.13 for total F and sea ice F, respectively. We chose these months to represent the MJ ICESat measurement periods.

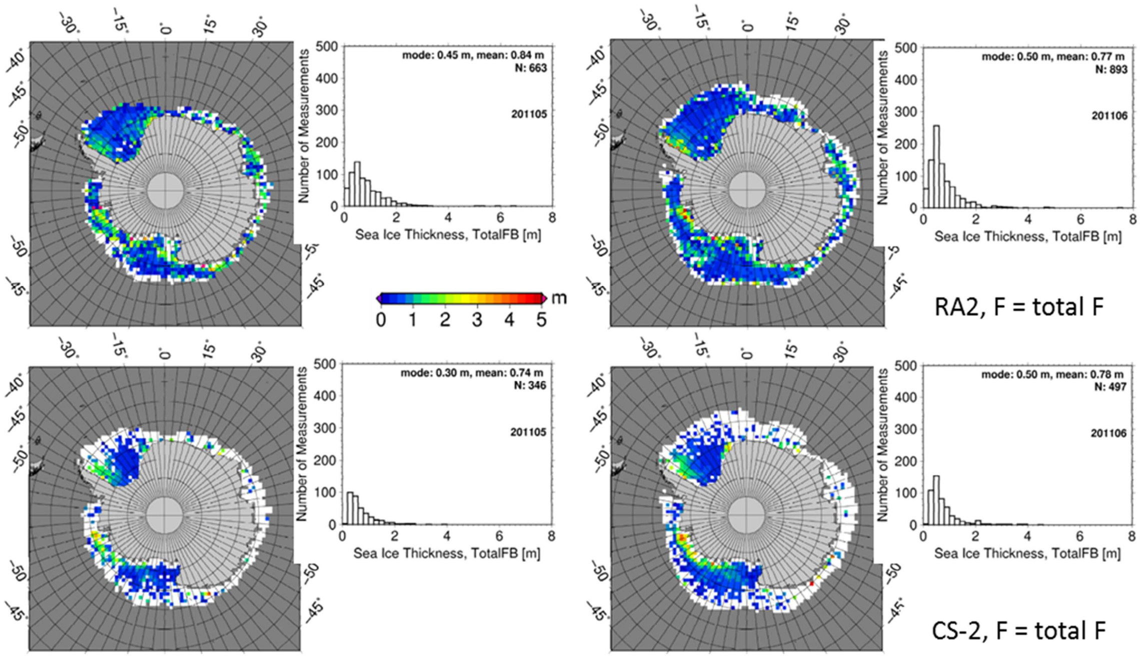

Figure 4.12: Sea ice thickness distribution around the Antarctic for Envisat RA2 (top) and CryoSat-2 (bottom) for freeboard case "total F" for months May (left) and June (right) 2011. White areas in the maps show grid cells with sea ice but without enough valid sea ice thickness data. Grid cell size is 100 km. Only grid cells with a sea ice concentration above 60% are shown. Each map is accompanied by a histogram showing the sea ice thickness distribution using bins of 0.2 m width. In each histogram the modal and mean sea ice thickness is given together with the number of valid data points N.

The sea ice thickness computed for case total F shown in Figure 4.12 is quite similar between RA2 (top) and CryoSat-2 (bottom). The distribution of thick and thin ice is similar. Sea ice thickness values hardly exceed 2 m; in particular the region East of the Antarctic Peninsula known to exhibit thick perennial ice does not contain ice thicker than 2 m. However, in some coastal grid cells in the Amundsen Sea both approaches provide ice thicker than 2 m. The histograms for June are very similar, share the same modal value: 0.50 m and an almost identical mean value: 0.77 m and 0.78 m. The histograms for May differ more; CryoSat-2 provides a lower modal value than RA2: 0.30 m versus 0.45 m and also the mean sea ice thickness is smaller by 0.1 m.

We note that there are substantially fewer grid cells with valid sea ice thickness values for CryoSat-2 than for RA2. In particular East Antarctic sea ice is under-represented in the CryoSat-2 sea ice thickness product.

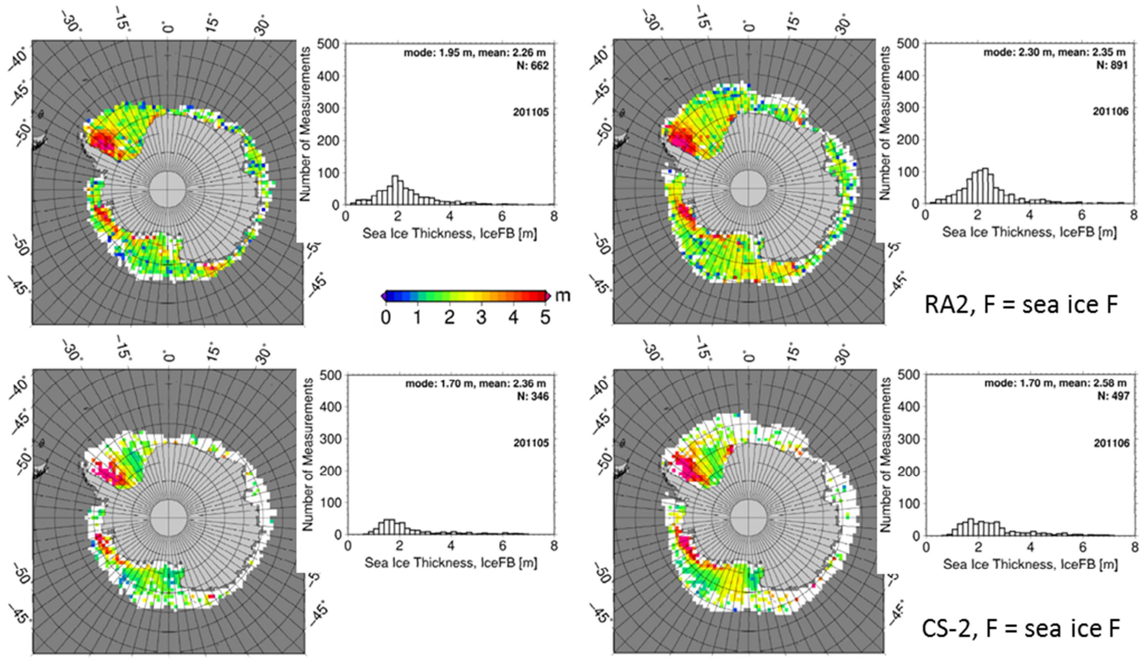

Figure 4.13: As Figure 4.12 but for freeboard case "sea ice F".

Figure 4.13 illustrates the May to June development of the sea ice thickness computed from RA2 (top) and CryoSat-2 (bottom) for the freeboard case "sea ice F". Sea ice thickness values are higher than for "total F" (Figure 4.12) by between 1.2 m and 1.8 m for the modal sea ice thickness and by between 1.42 m and 1.80 m for the mean sea ice thickness. Thickness values in regions known to be covered by perennial ice like the western Weddell Sea and in the coastal areas of the Amundsen / Bellingshausen Seas exceed 4 m for both RA2 and CryoSat-2. The two products differ, however, particularly for the modal sea ice thickness: RA2 has higher values by 0.25 m (May) and 0.60 m (June) than CryoSat-2. At the same time mean sea ice thickness values agree much better and within the mean sea ice thickness uncertainty (see Table 4.20 for RA2).

These sea ice thickness maps and histograms for May and June 2011 for both Envisat RA2 and CryoSat-2 (CS-2) for both freeboard cases "total F" and "sea ice F" helps to interpret the values shown in the following four tables. Here we show the all FM-period and all MJ-period average modal and mean sea ice thickness obtained with ICESat SICCI, RA2 total F and RA2 sea ice F for the ICESat periods listed in Table 2.1 in comparison to the values obtained with RA2 and CS-2 for the respective months using data from 2011. For FM we use February and March, and for MJ we use May and June. The aim is to relate the results obtained for 2011 to the results of the ICESat measurement period and identify / discuss potential differences.

Table 4.23: Modal sea ice thickness for ICESat period FM in comparison to the modal sea ice thickness from Envisat RA2 for case "Total F" and for case "sea ice F". In last column, the average modal sea ice thickness for February / March 2011 is given for Envisat RA2 as in the columns before and for CS-2; for both sensors the cases "Total F" and "sea ice F" are given.

Year	2004	2005	2006	2007	2008	Mean ± Stdv	2011
ICESat	0.90	1.10	0.70	0.90	0.90	**0.90 ± 0.14**	**--**
RA2, total F	0.50	0.50	0.45	0.45	0.50	**0.48 ± 0.03**	**0.50**
RA2, sea ice F	3.25	2.30	2.65	2.35	2.25	**2.56 ± 0.42**	**4.20**
CS-2, total F	--	--	--	--	--	**--**	**0.90**
CS-2, sea ice F	--	--	--	--	--	**--**	**4.28**

Table 4.24: As Table 4.23 but for the mean sea ice thickness for FM period.

Year	2004	2005	2006	2007	2008	Mean ± Stdv	2011
ICESat	1.38	1.82	1.78	1.62	1.38	**1.60 ± 0.21**	**--**
RA2, total F	0.69	0.88	0.94	1.11	0.89	**0.90 ± 0.15**	**0.78**
RA2, sea ice F	2.64	2.96	2.66	2.55	2.62	**2.69 ± 0.16**	**3.22**
CS-2, total F	--	--	--	--	--	**--**	**0.89**
CS-2, sea ice F	--	--	--	--	--	**--**	**3.99**

Tables 4.23 and 4.24 illustrate that for the FM period modal and mean sea ice thickness values obtained with RA2 total F for 2011 on the one hand and for 2004-2008 on the other hand agree within the bounds given by one standard deviation (over time). For RA2 sea ice F values found for 2011 exceed the all FM-period average as well as the individual modal or mean sea ice thickness values; the same applies to CS-2 sea ice F. CS-2 total F agrees with all FM-period average RA2 total F sea ice thickness for the mean but not for the modal value; the modal values agrees with the one obtained by ICESat though.

Table 4.25: Modal sea ice thickness for ICESat period MJ in comparison to the modal sea ice thickness from Envisat RA2 for case "Total F" and for case "sea ice F". In last column, the average modal sea ice thickness for May / June for 2011 is given for Envisat RA2 as in the columns before and for CS-2; for both sensors the cases "Total F" and "sea ice F" are given.

Year	2004	2005	2006	Mean ± Stdv	2011
ICESat	0.90	0.70	0.90	**0.83 ± 0.12**	**--**
RA2, total F	0.70	0.50	0.45	**0.55 ± 0.13**	**0.48**
RA2, sea ice F	2.50	2.10	1.95	**2.18 ± 0.28**	**2.13**
CS-2, total F	--	--	--	**--**	**0.40**
CS-2, sea ice F	--	--	--	**--**	**1.70**

Table 4.26: As Table 4.25 but for the mean sea ice thickness for MJ period.

Year	2004	2005	2006	Mean ± Stdv	2011
ICESat	1.21	1.41	1.38	**1.33 ± 0.11**	**--**
RA2, total F	0.90	0.95	0.96	**0.94 ± 0.03**	**0.81**
RA2, sea ice F	2.33	2.30	2.13	**2.25 ± 0.11**	**2.31**
CS-2, total F	--	--	--	**--**	**0.76**
CS-2, sea ice F	--	--	--	**--**	**2.47**

For MJ period modal sea ice thickness values obtained for 2011 and for 2004-2008 agree for both RA2 total F and RA sea ice F (Table 4.25). Corresponding values obtained with CS-2 are smaller but could still be considered as agreeing within the expected sea ice thickness uncertainty. Mean sea ice thickness values obtained with RA2 total F are out of the range given by one standard deviation while those obtained with RA2 sea ice F agree with the respective value obtained for 2004-2008 (Table 4.26). Mean CS-2 sea ice thickness values are smaller than RA2 total F for total F and larger than RA2 sea ice F for sea ice F, but again the difference is small: around 0.2 m and hence within the uncertainty margin.

As stated earlier, the accuracy of the modal values is not the best one when only a small number of grid cells is involved – like is the case for FM periods. We therefore can conclude from basically the MJ-period results that RA2 and CS-2 provide modal and mean sea ice thickness values for 2011 which agree within the expected value range due to the retrieval uncertainties – separately for freeboard case "total F" and "sea ice F".

In the following final two figures we show the difference CS-2 minus RA2 sea ice thickness for freezing period months April to September 2011. The aim is to identify potential areas where one or the other sensor provides substantially different sea ice thickness values. We again do this separately for both freeboard cases.

For freeboard case "total F" RA2 and CS-2 sea ice thickness values agree quite well with each other (Figure 4.14). The difference CS-2 minus RA2 sea ice thickness takes values mostly between -0.3 and 0.3 m (Figure 4.14). The distribution of the differences around the modal value which varies between 0.0 m (August) and 0.11 m (April) is almost symmetrical. The mean sea ice thickness difference is 0.0 m for April to June and around 0.08 m for July to September. These values are once again summarized in Tables 4.27 and 4.28 for the modal and the mean sea ice thickness differences, respectively, in the topmost row.

Table 4.27: Modal sea ice thickness difference CS-2 minus Envisat RA2 for January (month 1) to September (month 9) 2011 for "Total F" and "Sea Ice F". The last column denotes the number N of co-located grid cells. Values coinciding with Figures 4.14 and 4.15 are highlighted in bold font.

Month	1	2	3	4	5	6	7	8	9
Total F	0.26	0.38	0.41	**0.11**	**0.08**	**0.08**	**0.08**	**0.00**	**0.08**
Sea ice F	0.98	-0.20	0.98	**-0.10**	**0.00**	**0.23**	**0.53**	**-0.10**	**0.23**
N	24	33	87	**153**	**310**	**460**	**565**	**609**	**478**

Table 4.28: As Table 4.27 but for the mean sea ice thickness differences. N is the same as in Table 4.27 and is therefore omitted here.

Month	1	2	3	4	5	6	7	8	9
Total F	0.02	0.10	0.23	**0.00**	**0.00**	**0.00**	**0.09**	**0.07**	**0.07**
Sea ice F	0.94	0.65	0.52	**0.13**	**0.00**	**0.09**	**0.20**	**0.15**	**0.20**

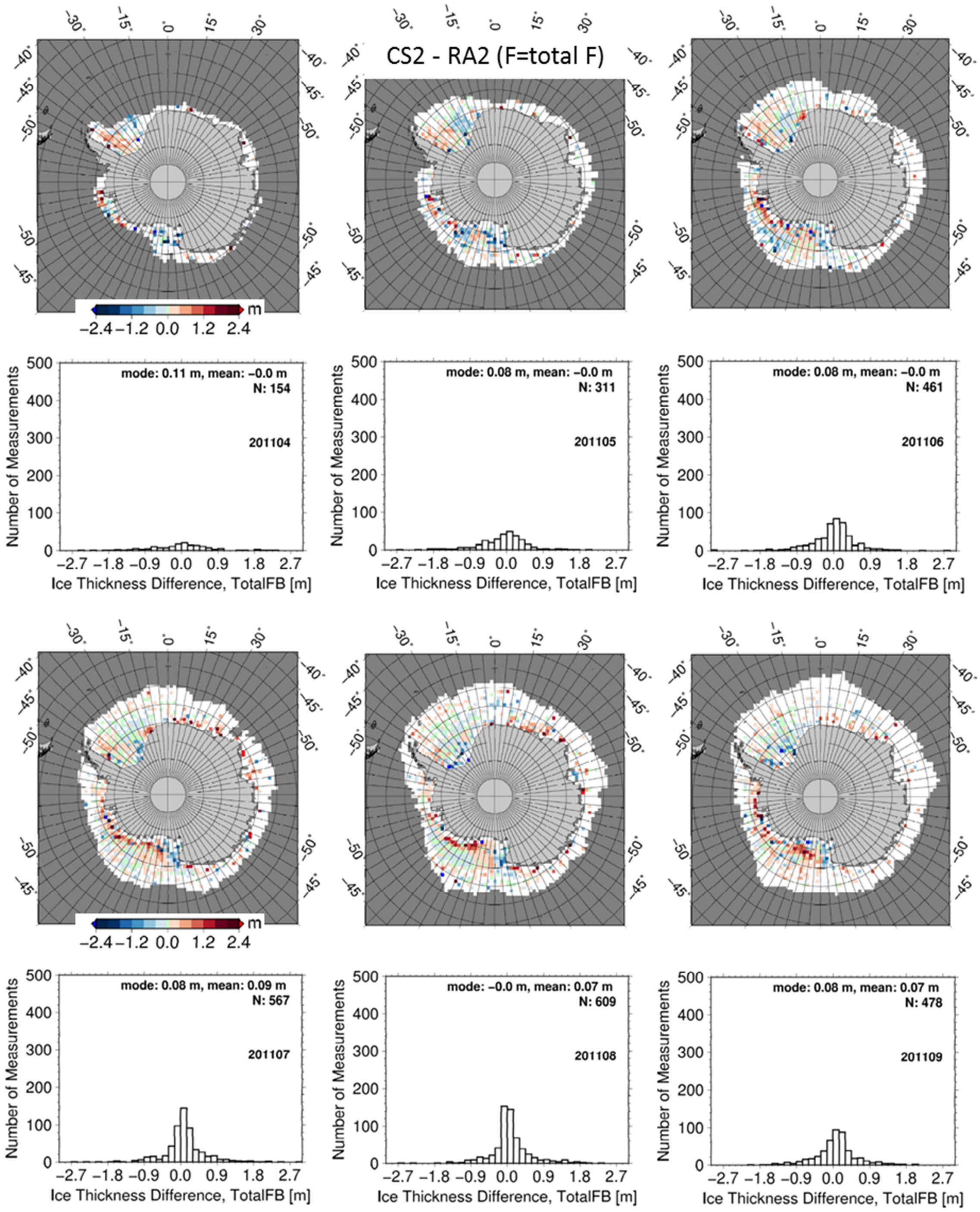

Figure 4.14: Difference in sea ice thickness CS-2 minus RA2 for freeboard case “total F” for April to June (top row) and July to September (bottom row) 2011. White areas in the maps show grid cells with sea ice but without enough valid sea ice thickness data. Grid cell size is 100 km. Only grid cells with a sea ice concentration above 60% are shown. Each map is accompanied by a histogram showing the sea ice thickness difference distribution using bins of 0.15 m width. In each histogram the modal and mean sea ice thickness difference is given together with the number of valid data points.

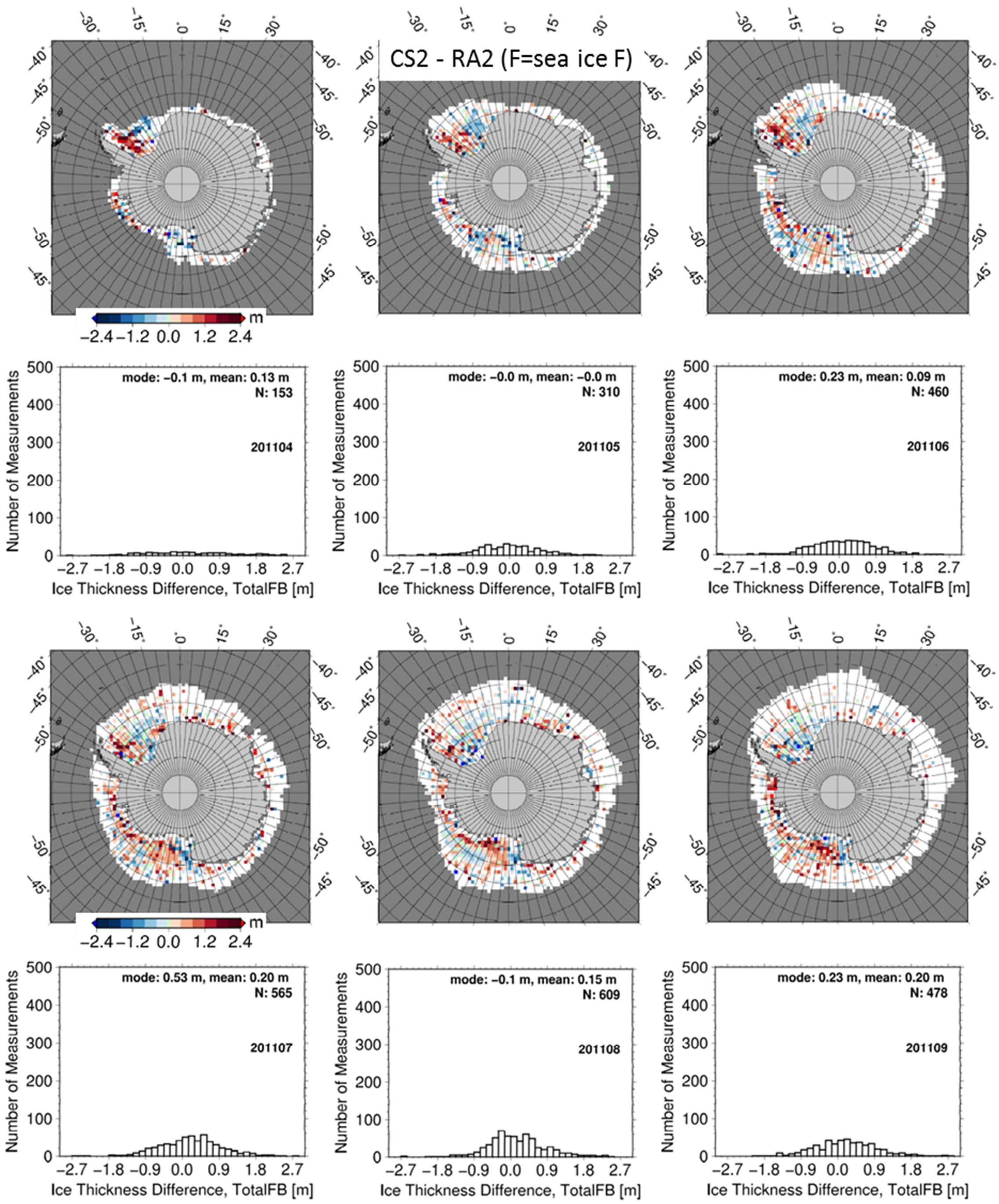

Figure 4.15: As Figure 4.14 but for the freeboard case "sea ice F".

Grid cells with a high (> 1.2 m) positive difference CS-2 minus RA2 sea ice thickness for total F (Figure 4.14) are mostly located near the coast (June, July) and also particularly in the southern Bellingshausen/Amundsen/Ross Sea (July, September). These are those areas where both approaches also tend to show thick sea ice. Grid cells with a high (< -0.8 m) negative difference CS-2 minus RA2 sea ice thickness are found most often in the southern Weddell Sea (July to September). In the Weddell Sea one can identify a dipole pattern with positive differences (CS-2 > RA2) in the West and negative differences (CS-2 < RA2) in the East (-30°E to -15°E) for April to June (Figure 4.14). This dipole vanishes as time elapses and is gone in August / September.

For freeboard case "sea ice F" RA2 and CS-2 sea ice thickness values agree clearly less well with each other than for case "total F" (compare Figure 4.15 with 4.14). The difference CS-2 minus RA2 sea ice thickness is more or less symmetrically centred around a modal value "around zero" but takes values from a considerably larger range: -0.9 to 0.9 m (Figure 4.15, histograms) than for case "total F" (Figure 4.14, histograms). Also "around zero" has to be understood in the sense that modal values range between -0.1 m and 0.53 m (see Table 4.27, middle row). Mean values of the sea ice thickness difference vary between 0.0 m (May) and 0.2 m (July, September) and hence are less variable than the modal values (see Table 4.28, bottom row). The concentration of sea ice thickness differences around 0 is much less pronounced than for "total F". This is nicely illustrated by both the histograms and the maps which show a large scatter of values between negative and positive differences.

The location of particularly large positive (CS-2 > RA2) sea ice thickness differences for "sea ice F" (Figure 4.15) is similar to those found for "total F" (Figure 4.14). However, the absolute values are considerably larger for "sea ice F" – particularly in the Weddell Sea (April to August). In some other regions, such as the southern Amundsen Sea the magnitude of these positive differences is the same though. As far as it concerns large negative (CS-2 < RA2) sea ice thickness differences both location and magnitude seem to be very similar for both freeboard cases. The dipole pattern in the Weddell Sea mentioned for case "total F" can also be identified for case "sea ice F" (Figure 4.15, May to July) and also vanishes as time elapses.

Table 4.29: April to September average modal and mean sea ice thickness difference CS-2 minus Envisat RA2 in meter together with one standard deviation.

April-September	Modal SIT	Mean SIT
Total F	0.07 ± 0.04	0.04 ± 0.04
Sea Ice F	0.13 ± 0.25	0.13 ± 0.08

Overall, averaging over all winter months (Figures 4.14 and 4.15, Tables 4.27 and 4.28, bold numbers) the modal and mean sea ice thickness difference CS-2 total F minus RA2 total F takes values of 0.07 m and 0.04 m, respectively. When considering the case "sea ice F" then these values are 0.13 m and 0.13 m, hence a bit larger than for case "total F" suggesting a small systematic positive bias of CS-2 compared to Envisat RA2.

4.4 Discussion of the results

The sea ice thickness maps and histograms produced for and shown in this report are based on measurements of three different satellite altimeters: ICESat-1 GLAS, Envisat RA2, and CryoSat-2 SIRAL. Envisat RA2 bridges between ICESat and CryoSat-2 (CS-2) which do not overlap in time. All these sensors provide a measure of an elevation relative to the water surface.

4.4.1 ICESat background

Measurements from ICESat are relatively straight-forward because it uses a laser altimeter. The laser pulse is reflected at the snow surface (or if no snow is present at the ice surface) with only little penetration into it. Hence the freeboard measured by ICESat, the so-called total freeboard is well defined. The largest uncertainty in the freeboard measurement, among satellite positioning error, uncertainties about the knowledge of the Earths' geoid, ocean tides, etc., is the limited accuracy with which the sea surface can be approximated from the ICESat measurements. The uncertainties related to this and to the other issues are discussed in Kwok et al. [2007], Kern and Spreen [2015] and in RD-03 and will not be discussed here. For the sea ice thickness retrieval we follow the approach suggested in Kern and Spreen [2015] and use 3 times the freeboard retrieval uncertainty.

4.4.2 Radar altimeter background

Measurements from the two radar altimeters Envisat RA2 (RA2 henceforth) and CS-2 are less straight-forward. Theoretically the main radar return is supposed to come from the ice-snow interface – provided that the snow is dry [Beaven et al., 1995]. Hence a radar altimeter is expected to measure the elevation of the ice-snow interface relative to the water surface, the so-called sea ice freeboard. Experimental work in both the Arctic and the Antarctic [Willatt et al., 2010; 2011] demonstrated that this is not necessarily the case – particularly for typical Antarctic sea ice. The results given in RD-05 are pointing into the same direction. Inter-comparison of in-situ measurements of total freeboard, the sea ice freeboard, and the snow depth and radar altimeter freeboard from both RA2 and CS-2 showed large discrepancies and suggested that there are cases where indeed the sea ice freeboard is measured but that the majority of the measurements seem to be closer to the total freeboard [RD-05; RD-09]. The discussion of potential uncertainties in radar freeboard is beyond the scope of this report and the reader is referred to RD-04 and RD-05. This ambiguity of what the radar freeboard represents led us to the strategy to take the radar freeboard as the sea ice freeboard and compute the sea ice thickness following Equation (9) (see Section 3.2) ***and*** to take the radar freeboard as the total freeboard and compute the sea ice thickness following the SICCI approach using Equations (1) and (2) (see Section 3.1).

Note that even though the SICCI CS-2 freeboard data set [RD-05] used in this report comes with a freeboard uncertainty we decided to not use it because the SICCI RA2 freeboard data set [RD-04] used in this report lacks freeboard uncertainty information. In order to have a fair comparison of both data sets when it comes to the freeboard-to-thickness conversion we assumed a freeboard uncertainty of 20% of the freeboard itself (see Section 3).

4.4.3 Grid resolution

We restricted our investigation to a grid resolution of 100 km. This is motivated by the grid resolution possible with the RA2 data, which is 100 km [RD-04]. All RA2 freeboard data used in this report have been provided at this grid resolution. In order to compare the sea ice thickness obtained from the three instruments properly we decided to use the same grid resolution for all of them. In principle, it is possible to use a grid resolution of 25 km for ICESat and also for CS-2; actually SICCI CS-2 freeboard has an original grid resolution of 25 km. But since ICESat and CS-2 do not have a temporal overlap, we did not see a pressing motivation to extend our investigations to data at a grid resolution of 25 km.

Because the SICCI sea ice thickness data set might compete with one published by Kurtz and Markus [2012] (KandM) we carried out a separate inter-comparison of these two approaches and here also looked at the two different grid resolutions: 100 km and 25 km. We comment generally on the comparison of these two approaches in subsection 4.4.4. Here we comment on the different grid resolutions. Tables 4.1 and 4.2 point out that, except for the modal SICCI sea ice thickness value of the MJ-periods, all FM-, MJ-, and ON-period average modal and mean sea ice thickness values obtained at the two different grid resolutions agree within one temporal standard deviation for SICCI and KandM. This is not the case for the difference ICESat minus KandM sea ice thickness (see Tables 4.3 and 4.4) which is, on average, larger at 100 km grid resolution than at 25 km grid resolution for both the modal and the mean difference. While for the all FM-period and the all MJ-period average modal sea ice thickness the value range given by one temporal standard deviation at 100 km grid resolution still includes the respective values obtained at 25 km grid resolution, those for ON-periods ar substantially different at the two grid resolutions – as exemplified for 2004 in Figure 4.16.

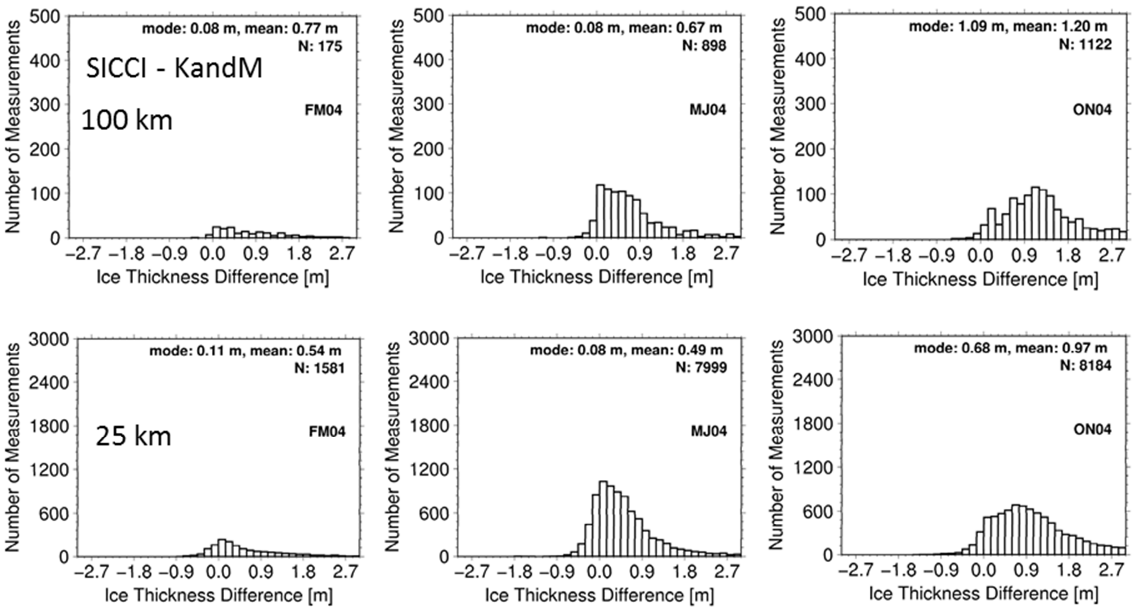

Figure 4.16: Histograms of the difference SICCI minus KandM sea ice thickness at 100 km grid resolution (top) and at 25 km grid resolution (bottom) for – from left to right – FM04, MJ04, and ON04. Bin size is 0.15 m. In each histogram the modal and mean sea ice thickness difference is given together with the number of valid data points. Note the different y-axis scaling because we have more grid cells at 25 km grid resolution.

In Figure 4.16 the modes for FM04 and MJ04 are similar but those for ON04 differ. The distribution of the differences seems to be broader for 25 km than for 100 km grid resolution. One indication for this is that all histograms for 25 km grid resolution have substantially more grid cells with negative differences than those for 100 km grid resolution. Intuitively one would expect that at 25 km grid resolution one gets a more realistic representation of the sea ice thickness differences which takes into account better the spatial variations in the sea ice thickness. However our results are kind of contradicting this view because a comparison of Tables 4.1 and 4.2 with Table 4.3 reveals that for both, 100 km and 25 km grid resolution the sea ice thickness differences one can compute from the values in Tables 4.1 and 4.2 agree better with the sea ice thickness differences computed at 100 km grid resolution. More detailed inter-comparison work is needed here. We note a few things here, however:

(1) SICCI and KandM sea ice thickness data are derived differently. Kurtz and Markus [2012] derive the data at 25 km grid resolution but they use kriging interpolartion to reduce noise and to interpolate between swaths. SICCI does not interpolate data. Single shot laser altimeter data are directly averaged into 100 km grid cells.
(2) The discrepancy cannot be caused by using snow depth data at different grid resolution because KanM do not use any snow depth (see Section 3.1).
(3) KandM barely provides sea ice thickness values above 2 m (see histograms in Figure 4.1).
(4) Using 25 km grid resolution reduces the number of days from which valid ICESat data of one ICESat measurement period are contributing to a sea ice thickness value of a particular grid cell. While at 25 km the bulk of the grid cells in, e.g. the Weddell Sea, get ICESat measurements from 1-2 days, at 100 km grid resolution this number increases to 3-4 days [RD-03].

4.4.4 General remarks about SICCI versus KandM

SICCI and KandM sea ice thickness data differ substantially. In general one can say that the KandM approach provides sea ice thickness values which are just half of the values computed with the SICCI algorithm (see Tables 4.1 and 4.2). The all ICESat-period average modal and mean sea ice thickness values obtained with KandM are 0.60 ± 0.24 m and 0.72 ± 0.13 m, respectively. The corresponding values obtained with SICCI are 1.05 ± 0.28 m and 1.62 ± 0.25 m.

Validation data for the ICESat measurement periods in the Antarctic are sparse. In the following we first mention a number of independent estimates of the all Antarctic mean sea ice thickness. These apply also to the other sections of the discussion and we will refer back to this subsection where applicable.

Worby et al. [2008] compiled an archive of ship-based visual observations of the sea ice thickness and snow depth on sea ice following the ASPeCt protocol. Summing over all seasons over the entire Southern Ocean over all ASPeCt data and taking into account the ridged ice fraction the mean sea ice thickness from these observations is 0.87 ± 0.91 m for 1982-2004. It is clearly stated, however, that it is likely that this value is biased low because a) ships tend to follow easy-to-navigate water and hence avoid the thickest ice and b) the method of estimating the ice floes' tilted by the ships' hull thickness by means of a ship-mounted scale bears some potential for missing loosely attached parts of the sea ice underneath the ice floe sliding away under the ice.

Ozsoy-Cicek et al. [2013] (OC2013) compiled sea ice thickness observations from 15 research cruises into the Southern Ocean over a period of 20 years (1988-2007). Their average sea ice thickness values is: 0.90 ± 0.35 m. The mean value agrees well with the value of Worby et al. [2008] (see above). The areas visited and sampled by these cruises are smaller than those covered by the ASPeCt observations, however, as the latter follow transects through the ice while the former are measurements carried out locally on single ice floes. The total number of profiles investigated by OC2013 is 174 the average length of the profiles is 50 m. It can be expected that careful positioning of the profiles did include several ridges so that this mean sea ice thickness value is not just from level sea ice. However, whoever experienced the pain of drilling a ridge for a sea ice thickness measurement knows that most likely most profiles were on level ice so that one could expect an under-estimation of the sea ice thickness in this data set as well. Also, the research cruise ships try to avoid heavy ice conditions so that it is likely that again the thicker parts of the sea ice thickness distribution are not represented by this data set and this mean sea ice thickness value – similar to Worby et al. [2008].

Sea ice thickness data exist from sea ice draft observations by upward looking sonar (ULS) in the Weddell Sea [Behrendt et al., 2013]. From the observations between the 1990ies until 2008 three main conclusions can be drawn:

(1) Sea ice draft (thickness) increases across the Weddell Sea from east to west towards the Antarctic Peninsula from about 1 m to about over 3 m (see also [Harms et al., 2001]);
(2) Sea ice draft (thickness) has a strong gradient towards the coast between about 5°E and -20°E with values between 0.5 m and 1 m at a few 50 km distance to the coast and values between 2 m and 3 m close to the coast.
(3) Along 0°E sea ice draft (thickness) slowly decreases northward from values between 0.5 m and 1 m to values around 0.5 m.

Helicopter-borne sea ice thickness measurements carried out in the western Weddell Sea (-53°E to -58°E; 67°S to 69°S) beginning of December 2004 [C. Haas, personal communication] revealed modal sea ice thickness values of 2.0 m for seasonal ice and 2.8 m and 3.5 m for perennial ice, obtained for subsets of 30 km length along the measurement track.

Sea ice thickness information given by the ASPeCt and the in-situ observations would favour KandM at first glance. However, inbetween the lines we can read that both independent data sources are most likely biased low which would bring these close to the SICCI all ICESat-period average modal sea ice thickness. Sea ice thickness provided by ULS and the helicopter-borne data confirm that sea ice thickness values exceed 2 m or even 3 m along region a): parts of the coast in the eastern Weddell Sea and in region b): east of the Antarctic Peninsula. KandM sea ice thickness does not provide any indication of a sea ice thickness gradient with substantially increasing sea ice thickness towards the coast in region a) while SICCI does (Figure 4.1). KandM sea ice thickness values in region b) reach 2 m but do not exceed this value while SICCI sea ice thickness values do exceed 2 m and even 3 m (Figure 4.1). On the other hand, KandM sea ice thickness estimates in the central and eastern Weddell Sea are between 0.3 m and

0.6 m and therefore agree somehow with the view given by the ULS observations.

What could cause these discrepancies between SICCI and KandM. The most obvious one is that KandM assumes that the sea ice freeboard is 0 cm everywhere. While this is an apropriate assumption in regions with thin, level, undeformed sea ice – as can be expected for the central eastern Weddell Sea – this assumption most likely fails in regions of i) thick level ice and ii) of deformed / ridged sea ice. In the latter cases an assumption of zero freeboard seems not to be justified. One could argue that this lack in agreement between algorithms' assumptions and actual conditions is the reason why, e.g., along the coast of the Eastern Weddell Sea (region a) KandM fails to provide thicker ice than in a few 50 km distance from the coast and why east of the Antarctic Peninsula (region b) KandM sea ice thickness values do not exceed 2 m. Kwok and Maksym [2014] presented Operation Ice Bridge (OIB) flight campaign results from several overflights of the south-western Weddell Sea and the southern Bellingshausen Sea in October 2010 and 2011. They discussed their findings in the context of the assumptions Kurtz and Markus [2012] made and came to the conclusion that the assumption of zero sea ice freeboard is potentially not justified along quite some portions of the OIB tracks investigated by them. This applies to both the Weddell Sea and the Bellingshausen Sea.

We would like to stress, however, that the assumption of zero sea ice freeboard still might be a reasonable thing to do – but it needs to go together with discrimination about where this assumption can be made and where not. The assumption of zero freeboard is, e.g., supported by the results of OC2013 who found an all Antarctic average sea ice freeboard of 2.4 ± 3.7 cm; above-mentioned concerns about the representativity of this data set apply here as well, though.

In a direct comparison and in the light of the available independent sea ice thickness information we dare to say that the SICCI approach provides – overall – more realistic sea ice thickness than KandM, particularly in those areas known to be covered by deformed sea ice and/or by thick sea ice with an applicable sea ice freeboard.

4.4.5 Positive / negative sea ice freeboard

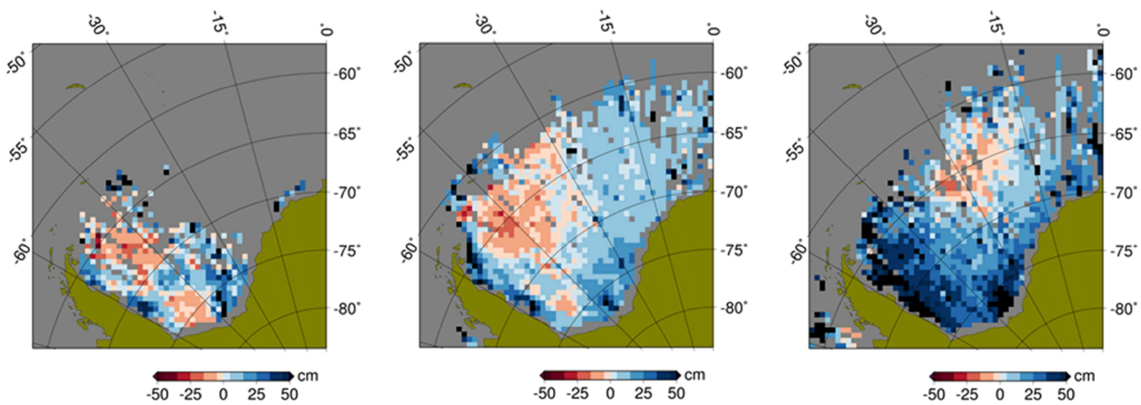

Figure 4.17: Difference ICESat total freeboard minus AMSR-E snow depth for ICESat periods – from left to right: FM04, MJ04, and ON04. Grid resolution is 50 km. Only grid cells with more than 60% ice concentration are shown.

The SICCI approach – or in general freeboard-to-thickness conversion algorithms using Archimedes principle and ICESat data in the way proposed by Kwok et al. [2007] require that the sea ice freeboard is positive. If this is not the case, e.g. if the snow depth is larger than the total freeboard then the sea ice freeboard would be negative and at a certain point one would retrieve negative sea ice thickness values. The work-around solution has been proposed by Zwally et al. [2008] and is also used in the SICCI algorithm.

Zwally et al. [2008], Yi et al. [2011] and also the SICCI approach identifies regions of negative sea ice freeboard by means of computing the difference ICESat total freeboard minus AMSR-E snow depth assuming that both data sets provide correct results. Figure 4.17 illustrates this difference for the ICESat measurement periods in 2004 for a part of the Weddell Sea. The bluish areas denote regions with positive sea ice freeboard while the red ones denote the areas with negative sea ice freeboard. These areas can occupy up to 40% of the total sea ice cover (see also [Yi et al., 2011]) and peak values are close to -0.2 m.

However, it is known that AMSR-E under-estimates the snow depth over deformed sea ice. Thick snow is therefore under-represented in the AMSR-E snow depth product used and hence cases with negative sea ice freeboard are potentially under-estimated. On the other hand once the sea ice is flooded, the ice-snow interface becomes wet as does the basal snow layer. Consequently – depending on the temperature gradient in the snow – snow metamorphism may occur, which could modify the physical snow properties. This modification can cause a substantially different radiometric signature of snow on flooded sea ice compared to dry snow on sea ice with a positive sea ice freeboard. Hence it is likely that the snow depth retrieval is not correct over flooded sea ice and depending on the dominant change of the snow properties, e.g. density change, grain size change, wetness change, the actual snow depth could be both over- or under-estimated. While the mentioned snow metamorphism is more likely to occur over flooded sea ice the generally small sea ice freeboard (see [Ozsoy-Cicek et al., 2013]) and the variable weather conditions can cause snow metamorphism also over sea ice with positive freeboard with a similar effect on the snow depth retrieval.

In short: The discrimination between positive and negative freeboard by means of ICESat total freeboard and passive microwave snow depth bears great potential for errors which cannot be quantified because the snow depth product accuracy as function of the mentioned snow property variation is also not (yet) quantified in the product used. The same applies to the new SICCI snow depth product which includes uncertainty information but this cannot reflect the variation in physical snow properties because the snow depth retrieval is an empirical one [RD-06; RD-07].

4.4.6 Different ICESat approaches

Apart from the KandM approach a number of different approaches have been tested. Two of the other approaches tested are like SICCI based on Archimedes principle. The one termed MandC (subsection 3.1.4) uses the climatological snow depth derived from SSM/I data [Markus and Cavalieri, 1998] which only depends on the season and provides a constant snow depth for the entire sea ice covered area. This approach is similar to SICCI, the only difference is the snow depth, i.e., it also includes the discrimination between positive and negative sea ice freeboards. The one termed Worby (subsection 3.1.5) is like OC2013 and KandM independent of the snow depth. Here the snow depth influence on the buoyancy of the sea ice is considered by using a reduced sea ice density. The reduction factor of the sea ice density is computed from the average seasonal sea ice thickness and snow depth values of Worby et al. [2008]. Both, MandC and Worby tend to provide – on average – larger sea ice thickness values than SICCI (Tables 4.5 to 4.10; Figures 4.3 to 4.5). Regional differences exist.

For FM04 (Figure 4.3), Worby has a considerably larger sea ice thickness in the Ross Sea than the other two approaches; here MandC and SICCI are similar. Also in the Weddell Sea the sea ice thickness distribution is more similar between MandC and SICCI than between Worby and SICCI; SICCI provides 1.5 m to 2.5 m, Worby 2 m to 3 m and MandC 2 m to 4 m sea ice thickness over most parts of the southern Weddell Sea. A comparison of Figure 4.3 with Figure 4.17, left image, suggests that the differences between SICCI and the other two approaches are particularly large where a negative sea ice freeboard is identified.

For MJ04 (Figure 4.4), all three approaches provide similar sea ice thickness values and distribution in the East Antarctic. In the Ross Sea, MandC and Worby agree with regard to the sea ice thickness distribution pattern while SICCI has a smaller thin ice area downstream of the Ross Ice Shelf polynya. A belt of thicker sea ice (around 1.5 m) is followed northward by a large area of thin sea ice (< 1 m); here both MandC and Worby show sea ice thickness between 1.5 m and 2 m. In the Weddell Sea also the sea ice thickness distribution pattern of MandC and Worby is almost identical; MandC provides much thicker sea ice along the Antarctic Peninsula, though: around 4 m versus around 3 m. For both approaches sea ice thickness values stay above 1.5 m up to -35°E. In contrast, SICCI sea ice thickness peaks at 3.5 m only very close to the Antarctic Peninsula and drops to values below 1 m already at -45°E. Also the area where the perennial sea ice is exported northwards and then north-eastwards is smaller in the SICCI sea ice thickness than in the other two approaches. Comparison with Figure 4.17, middle image, reveals that the region in the Weddell Sea where SICCI differs most from the other two approaches again is subject to negative sea ice freeboard values.

For ON04 (Figure 4.5), sea ice thickness distributions of MandC and SICCI are more similar. In particular the locations where both show large sea ice thickness values with 3 m to 4 m or even higher are similar. Worby shows elevated sea ice thickness values at these locations as well but the absolute values are smaller. Apart from that the sea ice thickness distribution is again similar for all three approaches – except of the patch with sea ice thickness < 1 m in the central Weddell Sea shown by SICCI but not by the other two approaches which give values around 2 m here. This patch coincides with the patch of negative sea ice freeboard in Figure 4.17, right image.

Both MandC and SICCI use passive microwave snow depth which is known to under-estimate actual snow depth over deformed sea ice [Worby et al., 2008b]. This was found out for East Antarctic sea ice first and confirmed later-on also for the Bellingshausen Sea [Kern et al., 2011]. In addition, it seems as if the to be expected seasonal increase in snow depth between early winter, i.e. MJ periods, and spring, i.e. ON periods, is not represented by passive microwave snow depth [RD-08]. On indication for this is also that the climatological snow depth used for MandC is 0.13 m in MJ and 0.13 m in ON, i.e. it does not increase over winter. If both these effects apply then it can be assumed that the snow depth used by MandC and SICCI for ON-periods is too low which – in view of Equation (1) means – that with a more realistic (higher) snow depth the retrieved sea ice thickness would be smaller – and hence more similar to the one provided by the Worby approach. The fact that many of the grid cells with particularly large sea ice thickness values are located close to the coast where deformation occurs regularly could be an indication that our hypothesis is correct. This is also supported by the independent data discussed in subsection 4.4.4. The large increase of the average modal and mean sea ice thickness from MJ to ON provided by SICCI and MandC of about 0.5 m (see Table 4.11) would be reduced under the influence of a more realistic (higher) snow depth. For an environment like the Southern Ocean with comparably large vertical oceanic heat fluxes an overall sea ice thickness increase by half a meter over winter seems to be a bit too high.

Whether or not the patches of negative sea ice freeboard shown in Figure 4.17 contribute to the differences between SICCI and the other two approaches remains to be investigated. No conclusion can be drawn here without independent information of the location of negative sea ice freeboard from other sources than a combination of ICESat and passive microwave snow depth. What can be said, however, is that in these regions with potential negative sea ice freeboard during MJ04 and ON04 (Figure 4.17) where MandC and SICCI show a substantial difference in the sea ice thickness (Figures 4.4 and 4.5), the climatological snow depth does equal the actual NSIDC AMSR-E snow depth. If they would be equal, then MandC and SICCI should show the same sea ice thickness because the approaches are identical – except for the snow depth used.

The other set of approaches is based on the empirical linear relationship between in-situ observations of sea ice thickness and total freeboard (OC2013). These have the advantage to be independent of information about snow depth and densities. The OC2013 approaches provide – on average – smaller sea ice thickness values than the three other approaches and values which are similar to those computed with KandM which has been discussed in Subsection 4.4.4. Because of this and because of the discussion carried out at the end of Subsection 4.1.3. we conclude that currently it is difficult and – based on the independent sea ice thickness information – unlikely that the OC2013 empirical approaches are able to provide accurate circum-Antarctic sea ice thickness. Also, using locally derived empirical relationships to compute sea ice thickness which locally agrees better to the actual sea ice thickness seems not be a straight-forward thing to do, because while with OC2013EA the sea ice thickness in the corresponding region: East Antarctic seems to be realistic with OC2013WWS the sea ice thickness in the corresponding region: western Weddell Sea is under-estimated (Figure 4.6 and Subsection 4.4.4).

4.4.7 Comparison ICESat to RA2 and CS-2

The fundamental difference between laser and radar altimetry is that they theoretically measure different elevations: total freeboard and sea ice freeboard, respectively. Since this seems not to be valid for the radar altimeter data used during the SICCI project [RD-04; RD-05] we computed sea ice thickness from the radar freeboard by assuming both possibilities: radar freeboard = total freeboard (case total F) and radar freeboard = sea ice freeboard (case sea ice F). Here we discuss the results.

Without exception the assumption that the radar freeboard is the sea ice freeboard yields sea ice thickness values considerably above those obtained with ICESat using the SICCI approach. Only for ON-periods the all ON-period average mean sea ice thickness obtained with case “sea ice F” is only about 0.20 m larger than the corresponding SICCI value. If one considers the other approaches used with ICESat data as well, then only MandC has an all ON-period average mean sea ice thickness which exceeds the case “sea ice F” value by about 0.2 m. Figure 4.18 illustrates the sea ice thickness for SICCI, MandC and Envisat RA2 sea ice F for MJ04 and ON04. This figure shows clearly that the assumption “sea ice F” provides sea ice thickness values of 2 m to 3 m all around Antarctic – regardless of whether we look at MJ04 or ON04. Apart from the fact that these values are presumably too high we also observe that the mean sea ice thickness decreases from MJ to ON for Envisat RA2 sea ice F (Tables 4.17 and 4.19). This is not the case for any of the sea ice thickness estimates based on ICESat data (Tables 4.5 to 4.10). Because all ICESat approaches show an increase in the mean sea ice thickness from MJ to ON, independent of whether they require snow depth for the freeboard-to-thickness conversion or not, we cannot relate this to the potentially too low snow depth in ON compared to MJ discussed in the previous subsection.

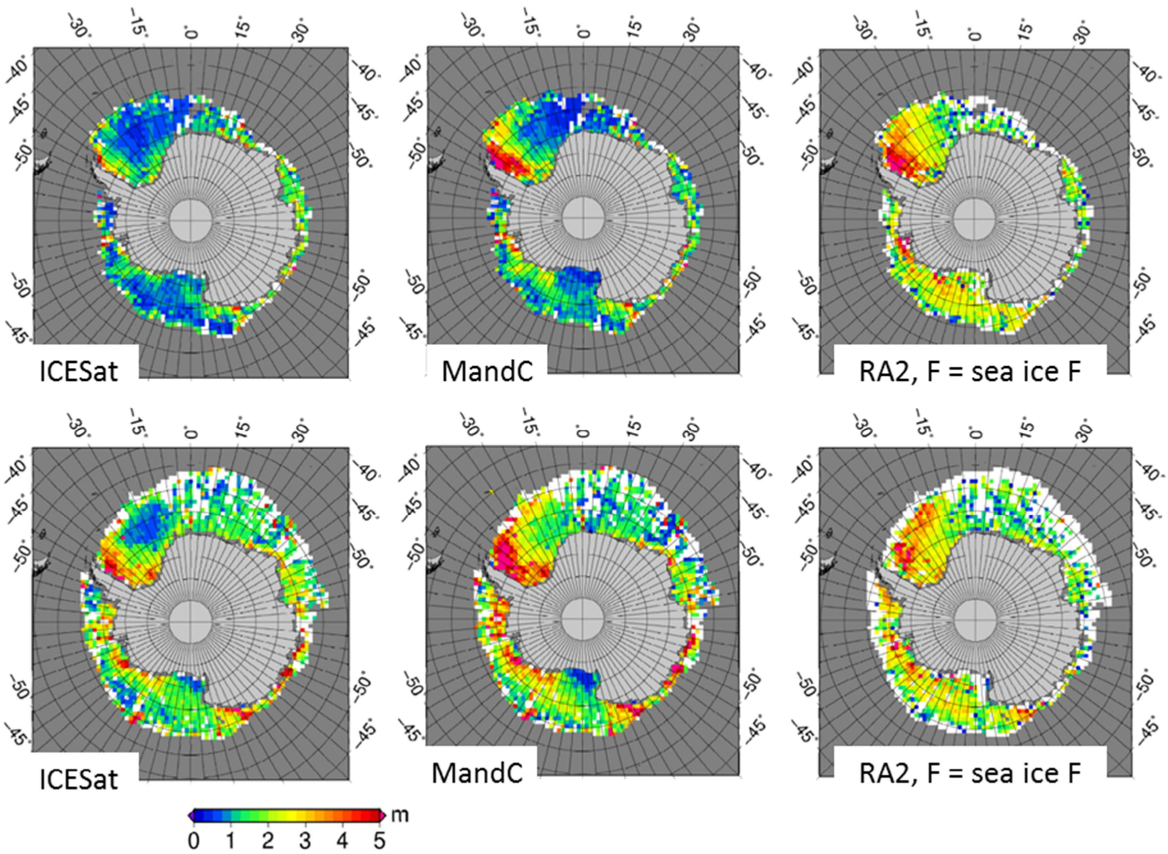

Figure 4.18: Sea ice thickness distribution around the Antarctic for ICESat SICCI (left) and MandC (middle) and Envisat RA2 sea ice F (right) for MJ04 (top) and ON04 (bottom). White areas in the maps show grid cells with sea ice but without enough valid sea ice thickness data. Grid cell size is 100 km. Only grid cells with a sea ice concentration above 60% are shown.

A possible hypothesis for the better agreement between Envisat RA2 sea ice F and ICESat SICCI or MandC sea ice thickness in ON compared to MJ could be that the snow properties during ON are more suitable to allow the radar altimeter to retrieve the actual ice-snow interface and hence the sea ice freeboard than the snow properties during MJ. Whether this hypothesis makes sense or not requires more investigations about the temporal changes of the snow properties on Antarctic sea ice during winter to spring. It seems to be rather unlikely that the presumably thicker but warmer snow pack during ON is drier and colder and contains less buried ice lenses or layers and is less vertically stratified than the thinner but colder snow pack during MJ. In contrast, the months October / November are associated with onset of melt or pre-melt conditions in some parts of the Antarctic snow cover [Willmes et al., 2009]. Under such conditions one would expect less penetration for radar waves at the frequencies used by RA2.

It is therefore more likely, that the main cause for i) the presumably too high Envisat RA2 sea ice F sea ice thickness and for ii) the unrealistic decrease of the mean sea ice thickness from MJ to ON lies in the radar freeboard retrieval and that a different re-tracker threshold might solve the problem [RD-04]. This applies also to CryoSat-2 (CS-2) which are shown to agree quite well with Envisat RA2 data (Section 4.3).

It does not seem that the other way of interpreting and using the radar freeboard, i.e. taking it as the total freeboard, does result in a realistic sea ice thickness distribution. First of all the mean sea ice thickness values are very low – comparable to ICESat KandM (see Figure 4.19). Secondly – even worse than KandM – the sea ice thickness distribution in regions such as the Weddell Sea does not resemble what is known, e.g. from Worby et al. [2008] or from ULS data [Behrendt et al., 2013] (see also Subsection 4.4.4). For example in MJ04 and ON04 Envisat RA2 total F sea ice thickness maps do not show the thicker perennial ice along the Antarctic Peninsula (Figure 4.19) which all ICESat sea ice thickness maps show (Figure 4.3 to 4.5).

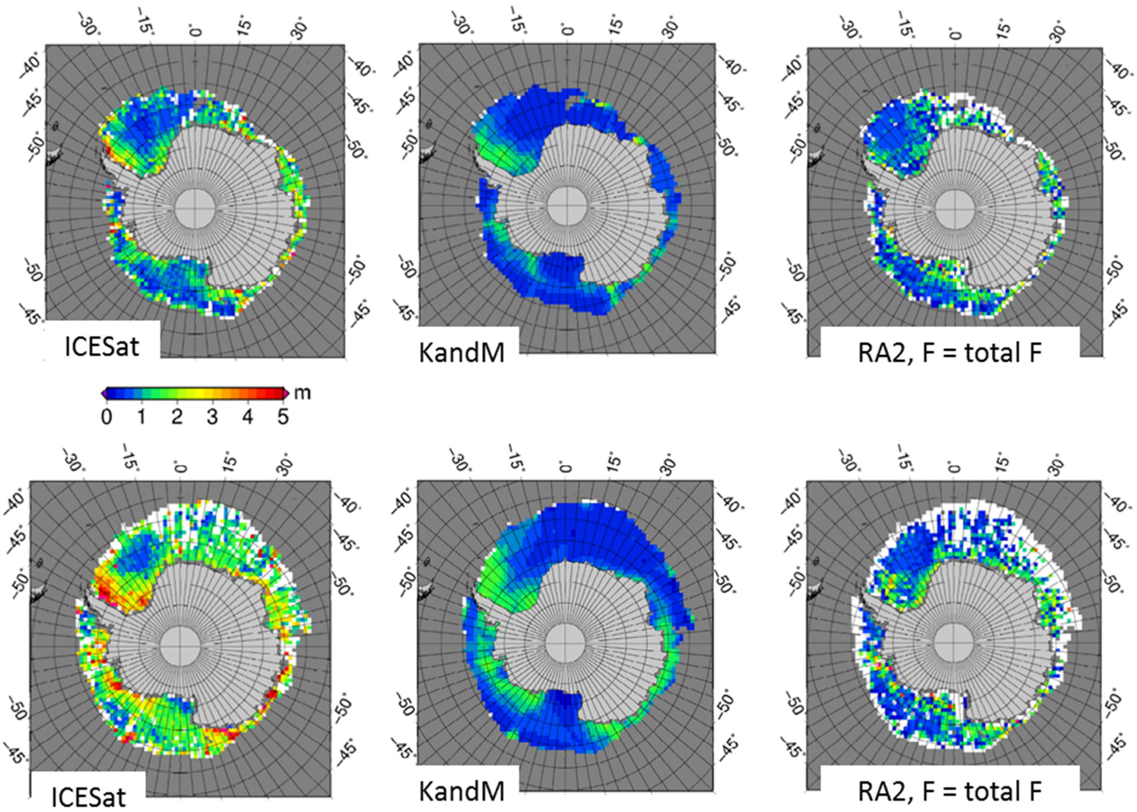

Figure 4.19: Sea ice thickness distribution around the Antarctic for ICESat SICCI (left) and KandM (middle) and Envisat RA2 total F (right) for MJ04 (top) and ON04 (bottom). White areas in the maps show grid cells with sea ice but without enough valid sea ice thickness data. Grid cell size is 100 km. Only grid cells with a sea ice concentration above 60% are shown.

We note in this context, however, that similar to the respective ICESat approaches we discriminated between positive and negative sea ice freeboard cases here. Now, because we can expect that – on average – the radar freeboard is below the ICESat freeboard (see also [RD-05]) it is more likely that the snow depth is larger than the radar freeboard and hence it is likely that more areas exhibit negative sea ice freeboard for Envisat RA2 total F than for ICESat.

The uncertainties arising from combing ICESat freeboard and passive microwave snow depth to identify regions subject to negative sea ice freeboard together with the fact that with Envisat RA2 total F we retrieve very low sea ice thickness values suggest that this "experiment" of interpreting radar freeboard as total freeboard cannot be recommended to be followed up with.

4.4.8 Impact of sea ice concentration

An impact of the different sea ice concentration data sets used (see Section 2.4) on the sea ice thickness retrieval can be excluded. First of all the sea ice concentration is only used as a threshold to discriminate between water and ice in the freeboard retrieval algorithms. At the spatiotemporal scales of interest: 100 km and monthly, it is unlikely that differences in the sea ice concentration between the data sets used – which can be assumed to be less than 10% - have an impact on the freeboard and/or freeboard-to-thickness conversion. Secondly, because the data investigated here are not weighed with the sea ice concentration but show the sea ice thickness of the sea ice in the respective grid cell as if it was covered with sea ice by 100%, any difference in the sea ice concentration data sets used also does not have an impact on our results.

5 Summary

Antarctic sea ice thickness was computed from ICESat laser altimeter and Envisat RA2 and CryoSat-2 radar altimeter data. For the radar altimeter data, which are supposed to represent the elevation of the ice-snow interface relative to the sea surface: the sea ice freeboard, two different approaches are used: the classical one, which takes the radar freeboard as a measurement of the sea ice freeboard, and another one, which takes the radar freeboard as a measurement of the total (sea ice + snow) freeboard; the total freeboard is the quantity measured by ICESat. For ICESat four different approaches which are based on Archimedes principle are used, two of which requires snow depth information while the other two allow freeboard-to-thickness conversion without additional snow depth information. For ICESat also a set of empirical approaches is used: linear regression equations based on in-situ measurement of total freeboard and sea ice thickness. This set also does not require any information about snow depth; in addition no information about the densities, like sea ice or snow density, is required. For ICESat and Envisat RA2 data sea ice thickness was computed for the ICESat measurement periods (see Table 2.1); for CryoSat-2 (and for comparison also for Envisat RA2) data sea ice thickness for months January to September 2011.

The results of all these approaches are inter-compared with each other where temporal overlap exists and with focus on the SICCI approach. The results are discussed in the view of the limited amount of independent sea ice thickness information available from other remote sensing sensors and/or ground-based observations.

These are the main conclusions which can be drawn:

(1) Compared to the radar altimeter freeboard data available within the ESA SICCI project at the time of writing this report ICESat based sea ice thickness has a greater potential to agree with current ideas about the absolute sea ice thickness and about the sea ice thickness distribution around Antarctica
(2) Avoiding the inclusion of snow depth information does not necessarily yield more realistic sea ice thickness values. This is demonstrated by an approach which assumes that the sea ice freeboard is zero everywhere, and hence sets snow depth equal to freeboard, and by the empirical approaches discussed.
(3) Independent sea ice thickness data based on in-situ measurements carried out during research cruises or based on ship-based visual estimations have to be utilized carefully. The thickest part of the sea ice thickness probability distribution is under-sampled by such observations because ships tend to follow easy-to-navigate sea ice and also measurements during research cruises are not always able to sample the sea ice in a representative way due to the difficulties of drilling through heavily deformed sea ice and (again) the need to avoid the thickest ice with the research ship.
(4) Of the ICESat data based approaches SICCI seems to have – averaged over all seasons – the best skills for obtaining a reasonable sea ice thickness distribution. The main caveats which need to be mentioned are i) the discrimination between positive and negative sea ice freeboard required needs to be validated; ii) the snow depth data set used currently is under-estimating snow depth for deformed sea ice and presumably also under-estimating the seasonal increase in snow depth over winter; both effects lead to an over-estimation of

the sea ice thickness during spring at places and to a too large seasonal increase in sea ice thickness over winter.

(5) One approach which avoids usage of the snow depth by incorporating the influence of snow on the sea ice buoyancy by a reduced sea ice density provides quite encouraging results and seems to be worth to be investigated further – together with regional empirical approaches.
(6) Envisat RA2 and CryoSat-2 sea ice thickness estimates agree with each other within the uncertainties computed; CryoSat-2 has a positive bias of about 0.1 m for winter (April to September) 2011.
(7) The radar freeboard data available from the ESA SICCI project under-estimate the sea ice thickness (absolute values and distribution) when the radar freeboard is taken as the total freeboard. In contrast, when the radar freeboard is taken as the sea ice freeboard – which is expected theoretically – the sea ice thickness is over-estimated. The general distribution between thicker and thinner parts of the sea ice cover seems ok though. What is interesting in this context is that taking the radar freeboard as the total freeboard gives better results for early winter while taking the radar freeboard as the sea ice freeboard gives better results in spring.
(8) Presumably the radar freeboard retrieval still has some potential for improvement so that it can be expected that a future version of the radar freeboard (SICCI-2) might agree better with both ICESat and independent sea ice thickness information.

Recommendations:

(1) Use the ICESat sea ice thickness prototype product provided in D1.9 carefully. It should be seen as a potentially more realistic distribution of the sea ice thickness around Antarctica than other data sets available and it comes with a grid-cell uncertainty estimate.
(2) Snow depth retrieval and quality assessment needs to be improved. In particular it is needed to quantify the impact of flooding and other processes changing the physical snow properties relevant for its remote sensing in the microwave frequency range on the snow depth retrieval quality. Currently snow depth retrieval is empirical.
(3) The currently used sea ice and snow densities need to be reviewed and potentially revised. There is more information available about Arctic sea ice and snow densities than in the Antarctic. Recent results from expeditions point to sea ice densities which might be considerably lower and more variable than thought before.
(4) Improvement of the radar freeboard data set particularly for fall and early winter seems to be a pre-requisite for a more realistic sea ice thickness obtained from radar altimetry in the Antarctic.

6 Literature

Beaven, S.G. and 8 others, Laboratory measurements of radar backscatter from bare and snow-covered saline ice sheets, Int. J. Remote Sens., 16(5), 851–876, 1995.

Behrendt, A., W. Dierking, E. Fahrbach, and H. Witte, Sea ice draft in the Weddell Sea, measured by upward looking sonars, Earth Sys. Sci. Data, 5, 209-226, doi:10.5194/essd-5-209-2013, 2013.

Cavalieri, D. J., T. Markus, and J. C. Comiso, AMSR-E/AQUA Daily L3 12.5 km Brightness temperature, sea ice concentration, and snow depth polar grids, V012, September 2002 to October 2011. NSIDC, Boulder, CO, Digital Media: http://nsidcc.org/data/ae_si12. 2004.

Comiso, J. C., D. J. Cavalieri and T. Markus, Sea ice concentration, ice temperature, and snow depth using AMSR-E data, IEEE Trans. Geosci. Rem. Sens., 41(2), 243–252, 2003.

Harms, S., E. Fahrbach, and V. H. Strauss, Sea ice transports in the Weddell Sea, J. Geophys. Res., 106, 9057-9073, 2001.

Kaleschke L, G. Heygster, C. Lüpkes, A. Bochert, J. Hartmann, J. Haarpaintner, and T. Vihma, SSM/I sea-ice remote sensing for mesoscale ocean–atmosphere interaction analysis. Can. J. Rem. Sens., 27(5), 526–537, 2001.

Kern, S., L. Kaleschke, and G. Spreen, Climatology of the Nordic (Irminger, Greenland, Barents, Kara and White/Pechora) Seas ice cover based on 85 GHz satellite microwave radiometry: 1992-2008, Tellus, 62A, 411-434, 2010.

Kern S., B. Ozsoy-Cicek, S. Willmes, M. Nicolaus, C. Haas, and S. F. Ackley, An intercomparison between AMSR-E snow depth and satellite C- and Ku-band radar backscatter data for Antarctic sea ice, Ann. Glaciol., 52(57), 279-290, 2011.

Kern, S., and G. Spreen, Uncertainties in Antarctic sea-ice thickness retrieval from ICESat, Ann. Glaciol., 56(69), 107-119, doi:10.3189/2015A0G69A736, 2015.

Kwok, R., G. F. Cunningham, H. J. Zwally and D. Yi, Ice, cloud, and land elevation satellite (ICESat) over Arctic sea ice: retrieval of freeboard, J. Geophys. Res., 112(C12), C12013, doi:10.1029/2006JC003978, 2007.

Kwok, R., and T. Maksym, Snow depth of the Weddell and Bellingshausen sea ice covers from IceBridge surveys in 2010 and 2011: An examination, J. Geophys. Res.-Oceans, 119, 4141–4167, doi:10.1002/2014JC009943, 2014.

Maksym, T., and T. Markus, Antarctic sea ice thickness and snow-to-ice conversion from atmospheric reanalysis and passive microwave snow depth, J. Geophys. Res., 113, C02S12, doi:10.1029/2006JC004085, 2008.

Markus T and D. J. Cavalieri, Snow depth distribution over sea ice in the Southern Ocean from satellite passive microwave data, In Jeffries MO ed. Antarctic sea ice: physical processes, interactions and variability. (Antarctic Research Series 74) American Geophysical Union, Washington, DC, 19–39, 1998.

Markus T, R. A. Massom R, A. P. Worby, V. I. Lytle, N. Kurtz, and T. Maksym, Freeboard, snow depth and sea-ice roughness in East Antarctica from in situ and multiple satellite data, Ann. Glaciol., 52(57), 242–248, doi:10.3189/172756411795931570, 2011.

Massom R. A., and 12 others, Snow on Antarctic sea ice, Rev. Geophys., 39(3), 413–445, doi: 10.1029/2000RG000085, 2001.

Meier, W., F. Fetterer, K. Knowles, M. Savoie, M. J. Brodzik. 2006, updated quarterly. *Sea Ice Concentrations from Nimbus-7 SMMR and DMSP SSM/I-SSMIS Passive Microwave Data*, [02-2004 to 03-2008]. Boulder, Colorado USA: National Snow and Ice Data Center, Digital Media, 2006.

Ozsoy-Cicek, B., S. F. Ackley, H. Xie, D. Yi, and H. J. Zwally, Sea ice thickness retrieval algorithms based on in situ surface elevation and thickness values for application to altimetry, J. Geophys. Res.-Oceans, 118, 3807-3822, doi:10.1002/jgrc.20252, 2013.

Spreen G, S. Kern, D. Stammer, R. Forsberg, and J. Haarpaintner J, Satellite-based estimates of sea-ice volume flux through Fram Strait. Ann. Glaciol., 44, 321–328, doi:10.3189/172756406781811385, 2006.

Spreen G, L. Kaleschke, and G. Heygster, Sea ice remote sensing using AMSR-E 89-GHz channels. J. Geophys. Res., 113 (C2), C02S03, doi: 10.1029/2005JC003384, 2008.

Willatt, R. C., K. A. Giles, S. W. Laxon, L. Stone-Drake, and A. P. Worby, Field investigations of Ku-Band radar penetration into snow cover on Antarctic sea ice, IEEE Trans. Geosci. Rem. Sens., 48(1), 365-372, 2010.

Willatt, R. C., S. W. Laxon, K. A. Giles, R. Cullen, C. Haas, and V. Helm, Ku-band radar penetration into snow cover on Arctic sea ice using airborne data, Ann. Glaciol., 52(57), 197-205, 2011.

Willmes, S., C. Haas, M. Nicolaus, and J. Bareiss, Satellite microwave observations of the interannual variability of snowmelt on sea ice in the Southern Ocean, J. Geophys. Res., 114, C03006, doi:10.1029/2008JC004919, 2009.

Worby, A. P., C. A. Geiger, M. J. Paget, M. L. Van Woert, S. F. Ackley, and T. L. DeLiberty, Thickness distribution of Antarctic sea ice, J. Geophys. Res., 113, C05S92, doi:10.1029/2007JC004254, 2008.

Worby, A. P., T. Markus, A. D. Steel, V. I. Lytle and R. A. Massom, Evaluation of AMSR-E snow depth product over East Antarctic sea ice using in situ measurements and aerial photography, J. Geophys. Res., 113(C5), C05S94, doi:10.1029/2007JC004181, 2008b.

Yi, D., H. J. Zwally, and J. W. Robbins, ICESat observations of seasonal and interannual variations of sea-ice freeboard and estimated thickness in the Weddell Sea, Antarctica (2003-2009), Ann. Glaciol., 52(57), 43-51, 2011.

Zwally, H. J., D. Yi, R. Kwok and Y. Zhao, ICESat measurements of sea ice freeboard and estimates of sea ice thickness in the Weddell Sea. J. Geophys. Res., 113(C2), C02S15, doi:10.1029/2007JC004284, 2008.

Zwally, H. J., and 7 others, GLAS/ICESat L2 sea ice altimetry data, Version 33 [Periods 2B to 3G]. National Snow and Ice Data Center, Boulder, CO. Digital media: nsidc/org/data/gla13, 2011.

< End of Document >